

# **International Ocean Discovery Program Expedition 372 Preliminary Report**

## **Creeping Gas Hydrate Slides and Hikurangi LWD**

**26 November 2017–4 January 2018**

Ingo A. Pecher, Philip M. Barnes, Leah J. LeVay, and the Expedition 372 Scientists



## Publisher's notes

Core samples and the wider set of data from the science program covered in this report are under moratorium and accessible only to Science Party members until 5 May 2019.

This publication was prepared by the *JOIDES Resolution* Science Operator (JRSO) at Texas A&M University (TAMU) as an account of work performed under the International Ocean Discovery Program (IODP). Funding for IODP is provided by the following international partners:

National Science Foundation (NSF), United States  
Ministry of Education, Culture, Sports, Science and Technology (MEXT), Japan  
European Consortium for Ocean Research Drilling (ECORD)  
Ministry of Science and Technology (MOST), People's Republic of China  
Korea Institute of Geoscience and Mineral Resources (KIGAM)  
Australia-New Zealand IODP Consortium (ANZIC)  
Ministry of Earth Sciences (MoES), India  
Coordination for Improvement of Higher Education Personnel (CAPES), Brazil

Portions of this work may have been published in whole or in part in other IODP documents or publications.

## Disclaimer

Any opinions, findings, and conclusions or recommendations expressed in this publication are those of the author(s) and do not necessarily reflect the views of the participating agencies, TAMU, or Texas A&M Research Foundation.

## Copyright

Except where otherwise noted, this work is licensed under the Creative Commons Attribution 4.0 International (CC BY 4.0) license (<https://creativecommons.org/licenses/by/4.0/>). Unrestricted use, distribution, and reproduction are permitted, provided the original author and source are credited.



## Citation

Pecher, I.A., Barnes, P.M., LeVay, L.J., and the Expedition 372 Scientists, 2018. *Expedition 372 Preliminary Report: Creeping Gas Hydrate Slides and Hikurangi LWD*. International Ocean Discovery Program.  
<https://doi.org/10.14379/iodp.pr.372.2018>

## ISSN

World Wide Web: 2372-9562

## Expedition 372 participants

### Expedition 372 scientists

#### Ingo A. Pecher

##### Co-Chief Scientist

School of Environmental and Marine Sciences  
University of Auckland  
New Zealand

[i.pecher@auckland.ac.nz](mailto:i.pecher@auckland.ac.nz)

#### Philip M. Barnes

##### Co-Chief Scientist

Ocean Geology  
National Institute of Water and Atmospheric Research (NIWA)  
New Zealand

[philip.barnes@niwa.co.nz](mailto:philip.barnes@niwa.co.nz)

#### Leah J. LeVay

##### Expedition Project Manager/Staff Scientist

International Ocean Discovery Program  
Texas A&M University  
USA

[levay@iodp.tamu.edu](mailto:levay@iodp.tamu.edu)

#### Sylvain M. Bourlange

##### Physical Properties Specialist

Laboratoire geoRessources-Ecole Nationale Supérieure de  
Géologie  
Université de Lorraine  
France

[sylvain.bourlange@univ-lorraine.fr](mailto:sylvain.bourlange@univ-lorraine.fr)

#### Morgane M.Y. Brunet

##### Sedimentologist

MARUM-Center for Marine Environmental Sciences  
University of Bremen  
Germany

[mbrunet@marum.de](mailto:mbrunet@marum.de)

#### Sebastian Cardona

##### Sedimentologist

Department of Geology and Geological Engineering  
Colorado School of Mines  
USA

[scardona@mines.edu](mailto:scardona@mines.edu)

#### Michael B. Clennell

##### Physical Properties Specialist/Downhole Measurements

Energy  
CSIRO  
Australia

[ben.clennell@csiro.au](mailto:ben.clennell@csiro.au)

#### Ann E. Cook

##### Physical Properties Specialist/Downhole Measurements

School of Earth Sciences  
Ohio State University  
USA

[cook.1129@osu.edu](mailto:cook.1129@osu.edu)

#### Brandon Dugan

##### Physical Properties Specialist/Downhole Measurements

Department of Geophysics  
Colorado School of Mines  
USA

[dugan@mines.edu](mailto:dugan@mines.edu)

#### Judith Elger

##### Physical Properties Specialist/Downhole Measurements

GEOMAR, Research Center for Marine Geosciences  
Christian-Albrechts-Universität zu Kiel (IFM)  
Germany

[jelger@geomar.de](mailto:jelger@geomar.de)

#### Davide Gamboa

##### Physical Properties Specialist/Downhole Measurements

British Geological Survey-Wales  
United Kingdom

[davide@bgs.ac.uk](mailto:davide@bgs.ac.uk)

#### Aggeliki Georgiopoulou

##### Sedimentologist

UCD School of Earth Sciences  
University College Dublin  
Ireland

[aggie.georg@ucd.ie](mailto:aggie.georg@ucd.ie)

#### Shuoshuo Han

##### Physical Properties Specialist/Downhole Measurements

Institute for Geophysics  
The University of Texas at Austin  
USA

[han@ig.utexas.edu](mailto:han@ig.utexas.edu)

#### Katja U. Heeschen

##### Organic Geochemist/Pressure Coring Specialist

GFZ German Research Centre for Geosciences  
Germany

[katja.heeschen@gfz-potsdam.de](mailto:katja.heeschen@gfz-potsdam.de)

#### Gaowei Hu

##### Physical Properties Specialist

Gas Hydrate Department  
Qingdao Institute of Marine Geology  
China

[hgw-623@163.com](mailto:hgw-623@163.com)

#### Gil Young Kim

##### Physical Properties Specialist/Downhole Measurements

Marine Geology and Exploration Center  
Korea Institute of Geoscience & Mineral Resources (KIGAM)  
Republic of Korea

[gykim@kigam.re.kr](mailto:gykim@kigam.re.kr)

**Hiroaki Koge****Physical Properties Specialist/Downhole Measurements**

Graduate School of Frontier Sciences/Atmosphere and Ocean  
Research Institute  
University of Tokyo  
Japan  
[koge@aori.u-tokyo.ac.jp](mailto:koge@aori.u-tokyo.ac.jp)

**Karina S. Machado****Organic Geochemist**

Production Engineering Department  
Federal University of Paraná  
Brazil  
[karinascurupa@gmail.com](mailto:karinascurupa@gmail.com)

**David D. McNamara****Physical Properties Specialist/Downhole Measurements**

Earth and Ocean Sciences  
School of Natural Sciences  
National University of Ireland, Galway  
Ireland  
[david.d.mcnamara@nuigalway.ie](mailto:david.d.mcnamara@nuigalway.ie)

**Gregory F. Moore****Physical Properties Specialist/Downhole Measurements**

Department of Geology and Geophysics/SOEST  
University of Hawaii at Manoa  
USA  
[gmoore@hawaii.edu](mailto:gmoore@hawaii.edu)

**Joshu J. Mountjoy****Sedimentologist/Structural Geologist/New Zealand Observer**

National Institute of Water and Atmospheric Research (NIWA)  
New Zealand  
[joshu.mountjoy@niwa.co.nz](mailto:joshu.mountjoy@niwa.co.nz)

**Michael A. Nole****Physical Properties Specialist**

Hildebrand Department of Petroleum and Geosystems  
Engineering  
University of Texas at Austin  
USA  
[michael.nole@utexas.edu](mailto:michael.nole@utexas.edu)

**Satoko Owari****Inorganic Geochemist**

Department of Earth Sciences  
Chiba University  
Japan  
[owari.stk@chiba-u.jp](mailto:owari.stk@chiba-u.jp)

**Education and outreach****Stephanie M. Sharuga****Education Officer**

National Oceanic and Atmospheric Administration (NOAA)  
USA  
[ssharuga@outlook.com](mailto:ssharuga@outlook.com)

**Matteo Paganoni****Physical Properties Specialist/Downhole Measurements**

Department of Earth Sciences  
University of Oxford  
United Kingdom  
[matteo.paganoni@earth.ox.ac.uk](mailto:matteo.paganoni@earth.ox.ac.uk)

**Paula S. Rose****Inorganic Geochemist**

Department of Physical and Environmental Sciences  
Texas A&M University-Corpus Christi  
USA  
[paula.rose@tamucc.edu](mailto:paula.rose@tamucc.edu)

**Elizabeth J. Sreaton****Physical Properties Specialist/Downhole Measurements**

Department of Geological Sciences  
University of Florida  
USA  
[sreaton@ufl.edu](mailto:sreaton@ufl.edu)

**Uma Shankar****Physical Properties Specialist/Downhole Measurements**

Department of Geophysics  
Institute of Science  
Banaras Hindu University  
India  
[umashankar@bhu.ac.in](mailto:umashankar@bhu.ac.in)

**Marta E. Torres****Inorganic Geochemist**

College of Earth, Ocean and Atmospheric Sciences  
Oregon State University  
USA  
[mtorres@coas.oregonstate.edu](mailto:mtorres@coas.oregonstate.edu)

**Xiujuan Wang****Physical Properties Specialist/Downhole Measurements**

Key Laboratory of Marine Geology and Environment  
Institute of Oceanology, Chinese Academy of Sciences  
China  
[wangxiujuan@ms.qdio.ac.cn](mailto:wangxiujuan@ms.qdio.ac.cn)

**Hung-Yu Wu****Physical Properties Specialist/Downhole Measurements**

Japan Agency for Marine-Earth Science and Technology  
Japan  
[sonata@jamstec.go.jp](mailto:sonata@jamstec.go.jp)

**Erin K. Todd****Education Officer**

Department of Geology  
University of Otago  
New Zealand  
[erin.todd@otago.ac.nz](mailto:erin.todd@otago.ac.nz)



## Operational and technical staff

### Siem Offshore AS officials

**Jacob C. Robinson**  
Master of the Drilling Vessel

**Mark Robinson**  
Drilling Supervisor

### JRSO shipboard personnel and technical representatives

**Robert Aduddell**  
Engineer

**Sandra Herrmann**  
Assistant Laboratory Officer

**Susan Boehm**  
Thin Section Laboratory

**Michael Hodge**  
Marine Computer Specialist

**Inva Braha**  
Curatorial Specialist

**Jon Howell**  
Applications Developer

**Ty Cobb**  
Physical Properties Laboratory

**Minh Huynh**  
Marine Computer Specialist

**Lisa Crowder**  
Assistant Laboratory Officer

**Rhonda Kappler**  
Publications Specialist

**Aaron de Loach**  
Core Laboratory

**Nicolette Lawler**  
X-Ray Laboratory

**Lachlan Douglass**  
LWD Engineer

**Aaron Mechler**  
Chemistry Laboratory

**Keith Dupuis**  
Underway Geophysics Laboratory/Downhole Tools Laboratory

**Mike Meiring**  
Engineer

**David Fackler**  
Applications Developer

**William Mills**  
Laboratory Officer

**Timothy Fulton**  
Senior Imaging Specialist

**Beth Novak**  
Paleomagnetism Laboratory

**Clayton Furman**  
Logging Engineer

**David Pedulla**  
LWD Engineer

**Randy Gjesvold**  
Marine Instrumentation Specialist

**Garrick Van Rensburg**  
Marine Instrumentation Specialist

**Kevin Grigar**  
Operations Superintendent

**Liam Warda**  
LWD Engineer

## Abstract

International Ocean Discovery Program (IODP) Expedition 372 combined two research topics, slow slip events (SSEs) on subduction faults (IODP Proposal 781A-Full) and actively deforming gas hydrate-bearing landslides (IODP Proposal 841-APL). Our study area on the Hikurangi margin, east of the coast of New Zealand, provided unique locations for addressing both research topics.

SSEs at subduction zones are an enigmatic form of creeping fault behavior. They typically occur on subduction zones at depths beyond the capabilities of ocean floor drilling. However, at the northern Hikurangi subduction margin they are among the best-documented and shallowest on Earth. Here, SSEs may extend close to the trench, where clastic and pelagic sediments about 1.0–1.5 km thick overlie the subducting, seamount-studded Hikurangi Plateau. Geodetic data show that these SSEs recur about every 2 years and are associated with measurable seafloor displacement. The northern Hikurangi subduction margin thus provides an excellent setting to use IODP capabilities to discern the mechanisms behind slow slip fault behavior.

Expedition 372 acquired logging-while-drilling (LWD) data at three subduction-focused sites to depths of 600, 650, and 750 meters below seafloor (mbsf), respectively. These include two sites (U1518 and U1519) above the plate interface fault that experiences SSEs and one site (U1520) in the subducting “inputs” sequence in the Hikurangi Trough, 15 km east of the plate boundary. Overall, we acquired excellent logging data and reached our target depths at two of these sites. Drilling and logging at Site U1520 did not reach the planned depth due to operational time constraints. These logging data will be augmented by coring and borehole observatories planned for IODP Expedition 375.

Gas hydrates have long been suspected of being involved in seafloor failure; not much evidence, however, has been found to date for gas hydrate-related submarine landslides. Solid, ice-like gas hydrate in sediment pores is generally thought to increase seafloor strength, as confirmed by a number of laboratory measurements. Dissociation of gas hydrate to water and overpressured gas, on the other hand, may weaken and destabilize sediments, potentially causing submarine landslides.

The Tuaheni Landslide Complex (TLC) on the Hikurangi margin shows evidence for active, creeping deformation. Intriguingly, the landward edge of creeping coincides with the pinch-out of the base of gas hydrate stability on the seafloor. We therefore hypothesized that gas hydrate may be linked to creep-like deformation and presented several hypotheses that may link gas hydrates to slow deformation. Alternatively, creeping may not be related to gas hydrates but instead be caused by repeated pressure pulses or linked to earthquake-related liquefaction.

Expedition 372 comprised a coring and LWD program to test our landslide hypotheses. Due to weather-related downtime, the gas hydrate-related program was reduced, and we focused on a set of experiments at Site U1517 in the creeping part of the TLC. We conducted a successful LWD and coring program to 205 mbsf, the latter with almost complete recovery, through the TLC and gas hydrate stability zone, followed by temperature and pressure tool deployments.

## Introduction

### Slow slip events

Slow slip events (SSEs) involve transient aseismic slip across a fault (lasting weeks to months) at a rate intermediate between the

plate boundary displacement rate and the slip velocity required to generate seismic waves. Only since the advent of dense, plate boundary-scale geodetic networks in the last decade has the importance of these events as a significant mode of fault slip been recognized. The observation of SSEs and associated seismic phenomena at subduction megathrusts worldwide (see review in Schwartz and Rokosky, 2007) has ignited one of the most dynamic fields of research in seismology today (e.g., Rubinstein et al., 2010; Peng and Gomberg, 2010; Wech and Creager, 2011). Although SSEs appear to bridge the gap between typical earthquake behavior and steady, aseismic slip on faults, the physical mechanisms that lead to SSEs and their relationship to destructive, seismic slip on subduction thrusts are poorly known. This deficiency in our understanding of SSEs is partly due to the fact that most well-studied subduction zone SSEs (Cascadia, southwest Japan) occur at too great a depth for high-resolution imaging or direct sampling of the source region. A notable exception is the northern Hikurangi subduction margin (HSM), New Zealand (Figure F1), where well-characterized SSEs occur every 2 years over a period of 2–3 weeks at depths <5–15 km below the seafloor (Wallace and Beavan, 2010; Wallace et al., 2016). The close proximity of SSEs to the seafloor at northern Hikurangi makes it feasible to drill into, sample, collect logs, and conduct monitoring within and around the source area in the near-field. Their regularity and well-characterized short repeat interval allow monitoring over multiple SSE cycles, with the potential to document the spatial and temporal distribution of strain accumulation and release, as well as any associated hydrogeologic phenomena.

The objectives of the International Ocean Discovery Program (IODP) Expedition 372 program include the collection of logging-while-drilling (LWD) data at three sites across the northern HSM. The LWD tools employed provided data on lithology, sonic properties, porosity, tectonic and formation hydrogeology, fault and wall rock microstructure, and stress conditions. Integration of the LWD data with seismic reflection data and with core data from IODP Expedition 375 will enable us to characterize the compositional, structural, thermal, hydrogeological, chemical, and diagenetic states, as well as the stress regime of the sedimentary and upper volcanic “inputs” section of the incoming plate, the shallow plate boundary fault near the trench, and the upper plate above the SSE source region. The data from the subduction inputs and frontal thrust sites will constrain the protolith and conditions in the updip part of the subduction fault zone associated with SSEs at greater depth.

The integrated log-core-seismic data will be used to identify borehole depth targets at the upper plate and frontal thrust sites for the installation of CORK observatories during Expedition 375 in 2018 (for further details, see Saffer et al., 2017). These observatories will span across the entire SSE source region and be used to monitor deformation, temperature, and fluid flow related to SSE cycles.

### Gas hydrates and submarine landslides

Submarine landslides constitute a significant geohazard and modify seafloor morphology (Mulder and Cochonat, 1996). Although progress has been made in studying their causes (Solheim et al., 2005), the processes that control the evolution of submarine slides are still only partially understood.

It is generally thought that submarine slides occur as single catastrophic events leading to mobilization and downslope transport of source material (Mulder and Cochonat, 1996). The submarine Tuaheni Landslide Complex (TLC) east of New Zealand’s North Island, however, exhibits features typical of active, slow-moving terrestrial earthflows that appear to be creeping rather than failing in

single events (Mountjoy et al., 2009). Such creeping behavior is observed on shore in mudslides (or earthflows) in weak clay-bearing rock (Baum et al., 2003) and in rock glaciers in ice-bounded sediments (Martin and Whalley, 1987). Intriguingly, at the TLC the creeping appears to be linked to the feather edge of gas hydrate stability (FEGHS) where the base of gas hydrate stability (BGHS) pinches out at the seafloor (Mountjoy et al., 2014b). Based on the curvature of bottom-simulating reflectors (BSRs) in the study area and BSR pinch-outs in the vicinity of the slides (Chiswell, 2005; Pecher et al., 2005, 2008), the FEGHS is predicted to be between 585 and 640 m water depth, which coincides with the upper limit of creeping interpreted from structural and geomorphic data.

At the FEGHS, gas hydrates, seafloor failure, and ocean change are critically intertwined (Phrampus and Hornbach, 2012). Because gas hydrate is known to strengthen sediments in short-term deformation tests, seafloor destabilization has been linked to hydrate dissociation, although there is no solid evidence for this process. We now suggest that the presence of gas hydrate itself may be implicated in creeping during long-term seafloor deformation.

## Background

### Tectonic setting

At the northern Hikurangi margin, the Pacific plate subducts beneath eastern North Island, New Zealand, at a rate of 4.5–5.5 cm/y (Wallace et al., 2004; Figure F1). The oceanic subducting plate comprises the Hikurangi Plateau, a rough-crust, seamount-studded large igneous province of Cretaceous age (120–90 Ma). The plateau is overlain by a Cenozoic to Mesozoic sedimentary sequence that thickens from ~1–1.5 km at northern Hikurangi (Figures F2, F3) to >5 km thick at southern Hikurangi, south of ~40°S. Thus, the northern Hikurangi margin is relatively sediment starved. This part of the margin is characterized by a mixed mode of spatially varying tectonic accretion and frontal tectonic erosion associated with subducting seamounts (Lewis et al., 1998; Collot et al., 2001; Pedley et al., 2010). The past subduction of seamounts may have an effect on fluid pressures at the plate interface (Bell et al., 2010; Ellis et al., 2015). A number of seamounts are present on the Pacific plate approaching the deformation front (e.g., Tūranganui Knoll [formerly Gisborne Knolls] and Puke Seamount). Where accretion occurs at northern Hikurangi, the margin is characterized by a narrow, steep (>10° taper angle) wedge geometry (Figure F3; Barker et al. 2009). The Hikurangi subduction thrust is identified as a décollement between an undeformed subducting sequence and a thrust-imbriated wedge. Barker et al. (2009) show that the interface lies <5–6 km below the seafloor 15–40 km from the trench. At the deformation front, the plate interface thrust is developed at about 5 km below sea level and about 2 km below the seabed, at least locally in the upper part of the Hikurangi Basement Sequence, which is thought to comprise volcanoclastics and/or chert/limestone rocks (Davy et al., 2008). The décollement position at northern Hikurangi is stratigraphically deeper than at the southern Hikurangi margin, where it is believed to occur in the inferred pelagic sequence above Paleogene carbonates (Barnes et al., 2010; Ghisetti et al., 2016).

### Slow slip events on the Hikurangi subduction margin

SSEs at the northern Hikurangi margin occur offshore of Gisborne township every 18–24 months and typically involve 1–2 cm of southeast surface displacement at continuously operating GPS (cGPS) sites (Figure F4) (Wallace and Beavan, 2010). The portion of

the subduction interface that undergoes slow slip is completely “locked” between the SSEs, and this locking or “slip deficit” is essentially fully recovered by slip in repeating SSEs (Wallace and Beavan, 2010). Inversion of cGPS displacements from these SSEs indicate that the equivalent moment magnitudes are typically Mw 6.5–7.0, with average slip of ~7–15 cm on the plate interface. These larger SSEs are punctuated by more frequent, smaller events (one or more per year) that are not as well characterized (cGPS time series inset in Figure F4). SSE slip near Gisborne predominantly occurs beneath the offshore region, with the downdip limit of slip near the coastline and repeated SSE rupture of the same areas of the interface (Wallace and Beavan, 2010). A recent seafloor geodetic experiment has shown that slow slip occurs to within at least 2 km of the seafloor beneath the Expedition 372 drilling transect, and it is possible that slow slip continues all the way to the trench (Wallace et al., 2016).

Multichannel seismic (MCS) data reveal regions where the interface (between <5 and >8 km depth) follows the top of a 1–2 km thick high-amplitude reflectivity zone (HRZ) in the subducting plate (Figure F3) (Bell et al., 2010). The January–February 2010 SSE coincided with the HRZ, whereas the subsequent March–April 2010 SSE source region lies within an intervening lower amplitude reflection zone. The high-amplitude reflectivity may be the result of high fluid concentrations within sediments entrained between downgoing seamounts. Alternatively, the reflections may result from altered oceanic basaltic lavas and volcanoclastics of the subducted Hikurangi Plateau. If the former interpretation is correct, then the correlation between the HRZ and SSEs suggests that fluids exert an important control on the generation of slow slip (Bell et al., 2010) by reducing effective stress (e.g., Kodaira et al., 2004; Liu and Rice, 2007; Audet et al., 2009; Song et al., 2009).

### Geologic setting of the Tuaheni Landslide Complex

The TLC is situated on the upper slope of the Hikurangi margin (Figures F2, F5). The outer shelf and upper slope are underlain by Quaternary shelf edge clinoform sequences (Pedley et al., 2010). These clinoforms consist of wedge-shaped sedimentary packages characteristic of sea level cycle–controlled progradational deposits (e.g., Posamentier and Vail, 1988; Van Wagoner et al., 1988). The clinoform sequences are fine grained at the surface (Alexander et al., 2010) but are likely to contain a significant sand fraction at depth like similar sequences in the vicinity (Barnes et al., 1991). Miocene and older rocks have been documented beneath the Quaternary sections; these sequences have been exposed at places following erosion and/or tectonic uplift (Field et al., 1997; Barnes et al., 2002; Mountjoy and Barnes 2011).

Dissociation of gas hydrates has long been proposed to be involved in seafloor failure, mainly because of (1) “melting” of a potentially frame-supporting or cementing solid to water and (2) net volume expansion leading to elevated pore pressure due to the generation of free gas (Kvenvolden, 1993; Mienert et al., 1998). Conversely, it has been implied that gas hydrate itself would strengthen sediments, as observed in a number of laboratory experiments (e.g., Winters et al., 2004; Priest et al., 2005). Most studies into the role of gas hydrates in seafloor instability have thus focused on the BGHS. A few recent findings, however, indicate that gas hydrates may directly or indirectly contribute to seafloor weakening. Rock Garden, a ridge on the Hikurangi margin with a flat top flanked by BSRs, appears to be eroded at the predicted top of gas hydrate stability in the ocean (Pecher et al., 2005). It has been proposed that gas hydrate indirectly causes seafloor weakening because a reduction of perme-

ability due to the presence of gas hydrate may lead to the buildup of overpressure and hydrofracturing of the seafloor (Crutchley et al., 2010; Ellis et al., 2010). Furthermore, although earlier laboratory tests suggest that gas hydrate itself, unlike ice, does not exhibit any viscous behavior (Durham et al., 2003), laboratory measurements on sands from the Nankai Trough indicate that gas hydrates may facilitate long-term deformation (Miyazaki et al., 2011). At the TLC, we see evidence that gas buildup and fracturing or viscous processes may occur in nature.

The TLC is thought to have initially formed as a catastrophic submarine slide (the parent slide) followed by ongoing slow deformation of the slide mass. The flanking by elongated strike-slip faults is evidence for slow deformation. The lower edge of the slide mass is unconfined. Morphology of faults in seismic data show compressional features in the upper part of the slide mass, whereas the lower part shows extensional features. These observations point toward a conveyor-belt model for sediment movement through the slides, where sediments are being supplied into the upper slide mass, leading to compression, and are being removed at the toe of the TLC, similar to mudslides and rock glaciers on land (Mountjoy et al., 2009).

It was originally suggested that slow deformation in the TLC reflects repeated small-scale seafloor failure associated with localized charging and discharging of pore pressure (Mountjoy et al., 2009) without involvement of gas hydrates. This process would lead to successions of small-scale compressional and extensional features.

We have, however, observed a general switch from compressional to extensional regimes at about 600 m water depth with compression above it and extension, indicating creeping, beneath it (Figure F6). This water depth coincides with the predicted FEGHS. We therefore hypothesize that gas hydrates may cause creeping in the TLC (Mountjoy et al., 2014b). The three proposed mechanisms behind creeping include sliding at the BGHS following gas hydrate dissociation, repeated “breaching” of a permeability boundary at the BGHS leading to transmission of pressure pulses beneath the creeping part of the slides (“hydrate pressure valve”), and viscous behavior of gas hydrate-bearing sediments (“hydrate glacier”) (Mountjoy et al., 2014b) (Figure F7).

### Seismic studies/site survey data

The key MCS data set available in support of the TLC drilling program was a P-Cable 3-D seismic reflection survey collected during Survey TAN1404 (Mountjoy et al., 2014a). Interpretation of these data, which were collected after publishing the hypotheses for active deformation, confirmed that the transition from a compressional to extensional (creeping) regime generally coincides with the predicted FEGHS. A possible décollement for creeping was identified 0.043 s two-way travelttime (TWT) beneath the seafloor (37 meters below seafloor [mbsf] assuming an average velocity of 1700 m/s; Mountjoy et al., 2016) (Figure F8).

These data were augmented by deep penetration high-fold seismic sections (Survey 05CM; up to 12 km streamer), low-fold (up to 48 channel) data collected by New Zealand research institutes during two surveys in 2011 (TAN1114) (Barnes and TAN 1114 Scientific Party, 2011) and 2012 (TAN1213), and low-fold high-resolution 2-D multichannel data acquired using the P-Cable seismic streamers collected during Survey TAN1404 (Mountjoy et al., 2014a). A long-offset seismic profile, which should provide improved velocity information across Site U1517 (proposed Site TLC-04B), was collected by the R/V *Marcus Langseth* (Cruise MGL 1708) as part of the SHIRE project shortly before Expedition 372.

## Previous drilling of the Tuaheni Landslide Complex

Two sites were drilled in April–May 2016 in the TLC to ~80 mbsf during the R/V *Sonne* Voyage SO-247 using the Meeresboden-Bohrgerät 200 (MeBo) robotic drilling system (Site GeoB20803 near proposed Site TLC-01D and Site GeoB20831 at Site U1517) (Huhn, 2016).

Site U1517 (Figure F8) was drilled to 80 mbsf with the MeBo in 2016 (Site GeoB20831) (Huhn, 2016), encountering deformed clayey silt in the upper 28 m and stiff clayey silt beneath 60 mbsf with good recovery. Between 28 and 60 mbsf, however, recovery with MeBo drilling was poor, yielding disturbed very fine sandy coarse silt. A second MeBo site was drilled ~100 m from our proposed alternate Site TLC-01D (Site GeoB20803), yielding similar lithologies with poor recovery in the upper part of the hole. MeBo drilling was not successful at recovering material across the interpreted décollement at ~40 mbsf in the seismic data. However, lithologies in the upper and lower parts of the MeBo cores were different, suggestive of a lithologic change across this interpreted décollement. Poor core recovery precluded pore water analysis for chlorinity as a gas hydrate proxy. MeBo drilling allowed borehole data to be tied to seismic reflections, particularly confirming the presence of intact sequences below landslide debris.

## Objectives

### Hikurangi subduction margin: hypotheses and scientific objectives

Drilling, downhole logging, coring, and instrumenting key sites will resolve competing hypotheses and key questions regarding the generation of SSEs and the mechanics of subduction interface thrusts. The major hypotheses that will be tested during Expeditions 372 and 375 are as follows:

- SSEs propagate to the trench. They are not confined to a specific (narrow) pressure or temperature range.
- Pore fluid pressure is elevated in the source region of SSEs. The elevated pore pressures are driven by mineral dehydration reactions that occur as sediments, and altered igneous crust on the incoming plate is buried by subduction or by disequilibrium compaction of low-permeability subducting sediments.
- SSEs occur in regions of conditional frictional stability. A single SSE fault patch can fail by multiple slip behaviors (e.g., steady creep, episodic slow slip, and seismic slip).
- There is a continuum of duration and magnitude characteristics of SSEs and slow seismic behavior on the shallow, updip section of the subduction zone.
- SSEs drive fluid flow along faults and throughout the upper plate.

To test these hypotheses, Expeditions 372 and 375 collectively will undertake the following coordinated strategy to accomplish the primary scientific objectives:

- Document the in situ conditions, material properties, and composition of the subduction inputs and the shallow plate boundary near the trench. These rocks comprise the protolith and reveal the initial conditions of fault rocks within the slow slip zone at greater depth. In the case of the shallow fault zone, these materials may in fact host SSEs if they propagate to the trench (Figure F4) (e.g., Wallace et al., 2016).



- Characterize the stress regime, temperatures, rock physical properties, lithologies, fluid pressures, fluid geochemistry, flow pathways, and structure of the upper plate above the SSE source.
- Install an array of borehole observatories across the upper plate that spans from the trench across the SSE source region to monitor hydrogeology, temperature, and pressure changes related to SSEs.

1. *HSM Objective 1: characterize the compositional, thermal, hydrogeological, frictional, geochemical, structural, and diagenetic conditions associated with the SSE source area.*

To achieve this goal, characterization of the incoming stratigraphy and upper oceanic basement rocks, together with the shallow most active strand of the frontal thrust system, is essential. A combination of LWD at Sites U1520 (proposed Site HSM-05A) and U1518 (proposed Site HSM-15A), located in the Hikurangi Trough and at a splay thrust fault, respectively, during Expedition 372 and coring during Expedition 375 will be used (Figures F9, F10). These activities will be followed by a strategy of carefully coordinated sampling and postexpedition laboratory analyses (e.g., Screation et al., 2009; Underwood et al., 2010). Site U1520 will target the entire sediment package on top of the Hikurangi Plateau. If conditions allow at Site U1520, drilling will penetrate into the top of the basaltic lava and/or volcanoclastic sequence. Site U1518 will provide LWD data and material from a frontal thrust in the updip region of the plate interface at low temperature and low effective stress. LWD during Expedition 372 will document continuous downhole trends in sediment properties and structure and will characterize stress conditions through analysis of wellbore failures (e.g., Chang et al., 2010). After LWD, coring during Expedition 375 will provide samples and data sets for sediment and rock physical properties, mineral composition, pore fluid composition, and downhole temperature, with a focus on hydrogeology and fault mechanical processes. In addition to Site U1520 in the Hikurangi Trough, Expedition 375 will also drill and core a second inputs site (proposed Site HSM-08A; see Saffer et al. [2017]) to target the upper (<200 m) altered basaltic basement of the Tūranganui Knoll Seamount massif (Figure F10). The LWD and core data from all inputs sites are also critical for refined depth conversion of the existing 2-D seismic data and 3-D seismic data collected by the *Marcus Langseth* shortly after Expedition 372. These data will also extend knowledge of in situ conditions (stress, fault zone properties, and pore pressure) away from the boreholes over a much broader region (Bangs and Gulick, 2005; Tobin and Saffer, 2009). Overall, this objective will constrain (1) the composition and frictional properties of subduction inputs updip of the shallow plate interface, (2) the hydrologic and thermal conditions of the incoming plate and shallow fault, and (3) the structural character, stress conditions, and mechanical properties of the main active thrust and subduction inputs.

2. *HSM Objective 2: characterize the properties and conditions in the upper plate overlying the SSE source region.*

The LWD data acquired during Expedition 372 will provide key information about fracture and faulting patterns and will allow us to evaluate the relationship between fractured intervals and any geochemical or thermal evidence of fluid flow in the upper plate above the SSE source region (e.g., Kopf et al., 2003). These data will also document borehole breakouts and/or drilling-induced tensile fractures, if present, to determine maximum and minimum horizontal stress orientations. In combination with rock physical properties data, this will be used to constrain stress magnitudes that may reflect variations in absolute strength of the plate boundary below

(e.g., Zoback et al., 2007; Lin et al., 2010; Chang et al., 2010). Downhole temperature will constrain thermal models of the margin needed to estimate the temperature structure and its relationship to slow slip and, ultimately, to estimate the loci of thermally driven dehydration reactions relative to SSE source regions (e.g., Saffer et al., 2008; Peacock, 2009). During Expedition 375, core samples collected from Site U1519 will enable measurements of rock elastic and physical properties needed to interpret observatory data and wellbore failures. Pore fluid analysis at Site U1519 will help to evaluate the source of fluids above and surrounding the region of SSE, which may flow upward and escape through the fractured and structurally disrupted upper plate (e.g., Kopf et al., 2003; Hensen et al., 2004; Ranero et al., 2008; Barnes et al., 2010). Core samples and downhole data from Site U1519 will provide critical physical and elastic properties information for the refined depth conversion of seismic data.

3. *HSM Objective 3: installation of borehole observatories spanning the SSE source region.*

For Objective 3: installation of borehole observatories spanning the SSE source region, refer to Saffer et al. (2017).

## Tuaheni Landslide Complex: hypotheses and scientific objectives

We planned to test the following hypotheses that may link gas hydrates to creeping:

- Hypothesis 1: overpressure may lead to slow sliding at the BGHS, in a modification of conventional models linking gas hydrates to seafloor instability (Phrampus and Hornbach, 2012; Figure F7A).
- Hypothesis 2: overpressure at the BGHS causes hydrofracturing, facilitating transmission of overpressure into the hydrate zone and sediment weakening, similar to mechanisms proposed for seafloor erosion on Rock Garden south of the TLC (Pecher et al., 2005; Crutchley et al., 2010) (hydrate pressure valve; Figure F7B).
- Hypothesis 3: interstitial gas hydrates in sediments within the TLC slide mass may cause creeping deformation, perhaps because of ice-like viscous behavior of hydrates (hydrate glacier; Figure F7C).

Antitheses (i.e., mechanisms that do not involve gas hydrates) include the following:

- Antithesis 1: creeping in the TLC could be caused by repeated small-scale failure associated with buildup and release of overpressure, the originally proposed mechanism behind creeping (Mountjoy et al., 2009).
- Antithesis 2: earthquake-related liquefaction of coarse silt beds, as detected during recent MeBo drilling, facilitates downslope movement.

Our program was designed to distinguish between the proposed hypotheses based on their following key manifestations:

- Hypothesis 1 (sliding at the BGHS): the key process controlling creeping would be elevated pressure at the BGHS. Temperature profiles will be important to reconstruct past pressure-temperature disturbances that may be causing ongoing gas hydrate dissociation and resulting overpressure.
- Hypothesis 2 (hydrate pressure valve): overpressure is present at the BGHS and transmitted into the gas hydrate stability zone.

The presence of a fracture network above the BGHS allows transmission of overpressure to the décollement, which facilitates creeping. No such fracture networks would be expected in the compressional part of the TLC.

- Hypothesis 3 (hydrate glacier): gas hydrate saturation would be expected to change across the décollement. Compressional and extensional parts of the slides would not show any significant differences in terms of pore pressure or fractures.

The antitheses would not predict any anomalies linked to gas hydrate saturation, in particular no pressure disruption at the BGHS or fracture networks related to gas hydrates. The two proposed mechanisms would otherwise have different signatures:

- Antithesis 1 (repeated small-scale seafloor failure): elevated pore pressure would be expected in the compressional regime (pressure charging) compared to the extensional zone (discharged).
- Antithesis 2 (liquefaction of coarse silt beds): cores might reveal localized shearing and liquefaction within the shear zone.

We planned to obtain the necessary data for distinguishing between our proposed creeping mechanisms by achieving the following objectives through drilling the TLC.

1. *TLC Objective 1: obtain lithologic information within the creeping slides, in particular across the proposed décollement of creeping.*

Coring was planned to obtain information on the lithology within the creeping, extensional part of the TLC and the underlying sediments. Recovering cores across the proposed décollement for creeping, from which MeBo drilling did not obtain any cores, was a high priority using the R/V *JOIDES Resolution's* advanced piston corer (APC) and half-length APC (HLAPC) systems. Lithologic information will be extrapolated using the seismic data.

2. *TLC Objective 2: collect samples for shore-based laboratory studies.*

The microscopic distribution of gas hydrate in sediments and its interaction with the sediment frame may be highly dependent on porosity distribution and mineralogy, such as clay minerals. We planned to test whether and how creeping may be linked to viscous behavior of the hydrate-sediment mix by conducting laboratory measurements on material recovered from the TLC. Sediments from APC, HLAPC, and, potentially, pressure cores at our site in the extensional regime (Site U1517) may be reconstituted followed by formation of gas hydrates. Alternatively, intact samples from the APC and HLAPC systems may be used for hydrate formation.

3. *TLC Objective 3: constrain in situ gas hydrate saturation and composition.*

Gas hydrate saturation with depth is a key parameter for all three proposed hydrate-related creep mechanisms. We planned to constrain profiles of gas hydrate saturation with depth based on LWD data and pore water chlorinity data from APC and HLAPC cores. Degassing of pressure cores was planned for additional calibration of gas hydrate saturation and for determination of the hydrate-forming gas composition. The gas composition is important for hydrate stability calculations and improved understanding of the general gas and gas hydrate system at the TLC. Furthermore, pore water profiles would provide information on fluid sources.

4. *TLC Objective 4: obtain pore pressure and temperature profiles.*

The hydrate pressure valve model and the model of sliding at the BGHS both involve pore pressure anomalies. Furthermore, the antithesis of repeated small-scale sliding at the BGHS without gas hydrate involvement is predicted to have a characteristic pressure signature. Pore pressure profiles are particularly important in the creeping extensional regime, where we planned a program using the temperature dual-pressure tool (T2P) to calibrate pore pressure. Emphasis will be on pore pressure changes across the proposed décollement and the BGHS. Temperature profiles are needed to constrain gas hydrate stability. Furthermore, changes in paleo-bottom water temperatures are a likely cause for gas hydrate dissociation leading to overpressure and sliding at the BGHS. Such bottom water changes would be reflected in anomalous temperature profiles with depth. We planned to measure seafloor temperatures with the third generation advanced piston corer temperature tool (APCT-3).

5. *TLC Objective 5: search for evidence of fracturing.*

The hydrate pressure valve model predicts transmission of pore pressure through fractures from hydraulic or pneumatic fracturing. We planned to constrain sediment fracturing as a function of depth at all three sites based on LWD data, particularly the resistivity images.

6. *TLC Objective 6: calibrate seismic data.*

Further quantitative analysis of the 3-D seismic data will aim at constraining potential lateral pressure variation along the décollement and deeper layers. Results from LWD sonic logs, tied with pressure profiles, will allow calibration of the seismic data. Furthermore, the LWD data may also provide critical shear wave calibration for long-offset seismic lines (MacMahon, 2016) and ocean-bottom seismometer site survey data (Wild, 2016) with the aim of extracting subsurface *S*-wave velocities using amplitude versus offset and *P*-to-*S* converted waves.

## Principal results

### Site U1517

Site U1517 is located in the extensional, creeping part of the TLC at ~720 m water depth (Figures F5, F6). The primary drilling objective was to use LWD and sample through the landslide mass and the gas hydrate stability zone to understand the mechanisms behind creeping.

Predrilling interpretation was based largely on high-resolution 3-D seismic site survey data collected in 2014. Initial data interpretation confirmed that, in general, the transition from a compressional to extensional (creeping) regime coincides with the predicted landward edge of the gas hydrate stability zone. The 3-D seismic cube provided detailed images of the architecture of the TLC, particularly a horizon within the debris mass that is interpreted to mark the décollement for the slowly deforming part of the TLC.

The following horizons were interpreted beneath the site (Figure F8):

- A possible décollement for creeping at 0.043 s TWT beneath the seafloor (37 mbsf for seafloor interval velocity of 1700 m/s),
- The base of the debris mass at 0.069 s TWT (59 mbsf), and
- The BGHS at 0.190 s TWT (162 mbsf).

The latter is mostly defined by the termination of high-amplitude reflections, although BSRs appear in patches along the level of the BGHS.

Site U1517 was previously drilled to 80 mbsf with the MeBo system (Site GeoB20831) during *Sonne* Voyage SO-247. The MeBo core revealed deformed clayey silt landslide debris between 0 and 28 mbsf with good core recovery. Between 28 and 60 mbsf, recovery was poor, yielding disturbed very fine sandy coarse silt in sections up to 1.5 m long (per 3.5 m stroke length). The cores were highly disturbed by the drilling process and mixed with seawater. From 60 to 78.8 mbsf, stiff clayey silt was sampled from within the bedded sedimentary sequence underlying the landslide complex with good core recovery.

Site-specific objectives include the following:

- Obtain lithologic information within the creeping slide. In particular, this includes material across the interpreted décollement for creeping and the lower part of the landslide debris.
- Collect samples for shore-based laboratory studies. Potential laboratory studies include long-term deformation tests on gas hydrate-bearing sediments and geotechnical and hydrogeological investigations of hydrate-bearing and hydrate-free sediments.
- Constrain in situ gas hydrate saturation and composition to better understand the local gas hydrate system and to calibrate seismic data.
- Analyze pore water profiles to improve calibration of gas hydrate saturation and to study possible fluid sources and chemical disequilibria.
- Obtain pore pressure and temperature profiles to investigate possible overpressure and search for evidence of non-steady-state fluid and heat flux.
- Identify fracturing and determine whether fracture patterns change across the BGHS or within the slide mass.
- Calibrate seismic data. Beyond stratigraphic tie ins, calibration of both 3-D and long-offset 2-D seismic data will improve constraints for extending profiles of gas hydrate saturation and pore pressure away from the borehole.

Hole U1517A was drilled to 205 mbsf with LWD starting on 16 December 2017. The vessel was offset by 20 m for Hole U1517B, which was abandoned because of uncertainties in the position of the mudline. Hole U1517C was drilled at the same location as U1517B for APC/HLAPC coring, reaching 188.5 mbsf. The vessel then left Site U1517 for completion of the remaining LWD program before returning to the site on 31 December to drill Hole U1517D for T2P/SETP deployments.

### Core lithology and structure

The lithostratigraphy in Hole U1517C is characterized as clayey silt with sandy intervals (Figure F11). We defined five lithostratigraphic units (I–V) based on visual description of core material, smear slide analysis, and red-green-blue (RGB) color and magnetic susceptibility logs. Smear slide analysis shows that Units I–IV have distinct characteristics with an overall decrease in grain size down-core from Unit I to IV, whereas Unit V includes a broad distribution of grain sizes. A variety of drilling-related core disturbance occurred, making robust interpretation of sedimentary structure challenging. Sedimentary structures, including sharp upper contacts and irregular basal contacts in graded beds, suggest that significant postdepositional modification of has taken place. Overall, we interpret this stratigraphic succession as including bedded turbidite se-

quences, mass transport deposits (MTDs), and background hemipelagic sedimentation. The upper ~67 mbsf are within the TLC and appear to be primarily an intact block that likely mobilized from the upper slope sedimentary sequences.

### Physical properties

Physical properties were characterized through a set of measurements on whole cores, split cores, and discrete samples. The magnetic susceptibility profile generally corresponds to the lithostratigraphic units, with sequences of sand and mud showing more variable magnetic susceptibility than laminated clay and silt or massive silty clay. Moisture and density (MAD) measurements on discrete samples from cores indicate relatively low porosity (~0.44) starting a few meters below the seafloor. A porosity shift occurs at 66 mbsf, with values increasing to 0.48. *P*-wave velocity and strength measurements on cores were compromised or prevented by expansion due to gas disturbance below 20 mbsf. Thermal conductivity measurements yield values averaging 1.2 W/(m·K) in the cored section. Fluctuations in thermal conductivity are small and appear inversely related to porosity, as expected based on the higher thermal conductivity of solids.

### Downhole measurements

The APCT-3 was deployed seven times in Hole U1517C. Four successful deployments between 81 and 132 mbsf define a linear temperature-depth profile with a gradient of 39.8°C/km. This gradient, combined with the average thermal conductivity measured on cores, yields an estimate of vertical conductive heat flow of 49 mW/m<sup>2</sup>.

Four attempts were made to measure in situ formation pressure and temperature in Hole U1517D. The T2P was deployed at 80 and 120 mbsf. The first deployment took a good formation pressure measurement. The second deployment may have collected good data, but it could not yet be retrieved because the electronics flooded. The SETP was deployed at 130 and 168.7 mbsf. Tool deployment and recovery went smoothly; however, the data file of the first measurement was erased from the memory card and the data file of the second measurement was corrupted. Efforts continue to convert the native data into a clean ASCII file.

### Logging while drilling

Hole U1517A recorded LWD data to the target depth of 205 mbsf (Table T1). Five LWD tools (NeoScope, SonicScope, TeleScope, proVISION, and geoVISION) were deployed on the bottom-hole assembly (BHA) while drilling Hole U1517A. These provided both real-time and recorded mode data through the TLC, below the décollement, and through the BSR. Based on the LWD measurements, five main logging units were identified that closely correspond to the lithostratigraphic units defined for Hole U1517C. Several significant features were interpreted from the logs, such as the compacted base of the debris flow from 54 to 60 mbsf and natural gas hydrate occurring in 10–30 cm thick turbidite sands from 110 to 150 mbsf. Both conductive and resistive fractures were also identified throughout the hole; however, a higher fracture density occurred within the landslide complex.

### Geochemistry

We collected 75 whole-round samples for characterization of the pore water in Hole U1517C. Samples were collected on the catwalk at a frequency of four samples per core in the upper 15.2 mbsf and two samples per core from 15.2 to 112.4 mbsf. Below this depth, sample selection was guided by cold anomalies observed in infrared



camera images that suggested the potential for gas hydrate occurrence. Additional samples were taken away from the cold anomalies to establish the in situ background chloride concentrations. Dissolved chloride measurements indicate the presence of discrete gas hydrate occurrences between ~135 and 165 mbsf, with gas saturation ( $S_h$ ) values ranging from 2% to 68%. This distribution is consistent with inferences on gas hydrate saturation based on resistivity data obtained by LWD. When it was possible to isolate thin dark coarse silt layers from the background fine clay matrix, we analyzed each lithology separately. Within these separated samples, gas hydrate in the fine clay layers that were immediately in contact with the gas hydrate-bearing, coarse-grained layers ranged from nondetectable to 2%, whereas the thin coarse layers within the whole round host gas hydrate at saturations ranging from 5 to 50%. This illustrates the preferential occurrence of gas hydrate in the coarse-grained material.

Pore fluid composition reflects the combined effects of microbially mediated organic matter degradation coupled to carbonate and silica diagenetic changes. The sulfate–methane transition (SMT) is well defined at 16.6 mbsf by depletion of dissolved sulfate and a marked increase in methane concentration in headspace samples. Alkalinity, calcium, and magnesium show distributions that are typical for reactions occurring at the SMT.

Below the SMT, methane concentrations rapidly increase to as much as 1%, indicating ongoing methanogenesis. The measured methane concentrations below the SMT are close to or above pore water saturation at ambient conditions. These values are qualitative estimates only because they reflect the amount of gas remaining in the sediment after core recovery and handling rather than the original values.

Ethane was not detected in the headspace samples above 146 mbsf, but it was repeatedly measured at very low concentrations of 1–2 parts per million by volume (ppmv) between 146 and 166 mbsf, a depth range that coincides with the inferred presence of gas hydrate from the chloride data.

Pore water profiles in the methanogenic zone suggest a combination of reactions that may include silicate weathering and formation of authigenic minerals that remove iron, manganese, calcium, and potassium from the pore water.

Analyses of the solid phase yielded  $\text{CaCO}_3$  values ranging from 4.63 to 8.99 wt% (mean =  $6.52 \pm 1.13$  wt%). Total organic carbon concentrations are generally <1% with slightly higher concentrations in lithostratigraphic Unit IV (mean =  $0.71 \pm 0.16$  wt% organic carbon within this unit) and a few measurements that reached 1.68 wt% in Unit V. The C/N ratios ranged from 3.78 to 31.34 (mean =  $9.46 \pm 3.52$ ) with variations that suggest higher heterogeneity of the organic matter in lithostratigraphic Units II and V.

### Log-seismic integration

LWD logs were tied to seismic profile In-line 1778 of the Tuaheni 3-D seismic volume through a set of synthetic seismograms (Figure F11). Two sets of synthetics were constructed. One set edited the LWD density and sonic logs to calculate acoustic impedance logs that were convolved with a wavelet derived from the seafloor of the seismic data. The other set used a log-lithologic model of the main lithostratigraphic units and physical properties. Washouts due to silty/sandy lithologies led to relatively poor quality density and sonic logs. Therefore, the synthetic seismograms did not match well. However, the main lithostratigraphic and logging units were tied to the primary seismic reflection units and their boundaries. The mismatches in depth between the seismic and log

data allowed us to refine the velocity profile at the drill site in order to reconvert the depth section.

### Core-log integration

By integrating LWD data taken in Hole U1517A and cores from Hole U1517C, we compared lithologic indicators (natural gamma radiation [NGR], sonic  $P$ -wave velocity, porosity, and bulk density) and independent estimates of gas hydrate accumulation (pore water geochemistry and resistivity–porosity relationships). Whole-round NGR measurements are in agreement with those taken through LWD. Additionally, core sample–derived MAD porosities agree well with measured LWD nuclear magnetic resonance (NMR) LWD porosities, but MAD measurements are consistently lower than the LWD neutron porosity measurements (Figure F11). Furthermore, there appears to be a slight mismatch in the depths at which significant changes in measurement responses occur: in the shallow section above 70 mbsf, excursions from baseline values appear approximately 5 m lower in core data than LWD data. This observation is consistent across both the NGR and porosity measurements, but the trend is difficult to distinguish deeper in the wells. Hydrate saturation was estimated using LWD-based methods and core geochemistry analysis. These techniques agree in their assessment of the most probable areas of hydrate occurrence but disagree in their predictions of hydrate saturation magnitude, likely due to differences in sampling resolution and formation heterogeneity.

## Site U1518

Site U1518 is located on the lower continental slope approximately 62 km from shore (Figures F2, F9). The site lies on the frontal accretionary wedge about 6.5 km west of the deformation front at 2636 m water depth. Site U1518 targeted a major west-dipping thrust fault that ramps from the interplate thrust and reaches the seafloor along an escarpment about 500–1000 m east of the drilling site (Figure F3). The geological and contemporary rate of activity on the thrust has not yet been established, but predrilling estimates suggest it may accommodate a significant proportion of the plate convergence across the margin. Seafloor geodetic data indicate that SSEs on the interplate thrust farther west extend off shore (trenchward) into the vicinity of Site U1518.

The primary objective at Site U1518 during Expedition 372 was to acquire LWD data to help characterize the structure and location of the shallow part of the fault and the nature of the sedimentary sequences that host it. These data will be integrated with proposed cores from this site planned for Expedition 375, and both types of data will be used to identify suitable formations and fault rock for hosting a borehole observatory planned for installation during Expedition 375. With very shallow SSEs on this northern segment of the Hikurangi margin recurring every 1.5–2.0 years, it is anticipated that the borehole observatory will record pressure, temperature, and fluid flow transients associated with SSE-propagated strains within the frontal accretionary wedge.

Based on predrilling interpretation of the seismic data at Site U1518, the thrust fault was expected to lie between 295 and 325 mbsf. The hanging wall sequence (i.e., the sediment above the fault) was expected to include 65–82 m of moderately reflective sediment, overlying a relatively weakly reflective interval characterized by irregular reflections and assumed to be Plio–Pleistocene in age. The hanging wall sequence apparently dips easterly within the forelimb of an anticlinal fold associated with the thrust fault. The footwall sequence (i.e., below the fault) to the 600 mbsf target drilling depth was expected to include a relatively strongly reflective interval at



least 70 m thick immediately below the fault that overlies a relative weakly reflective lower sequence. The entire footwall sequence drilled has an apparent westerly dip on the seismic profile, and at depths above 600 mbsf, it is inferred to be Plio–Pleistocene in age. The entire borehole was expected to encounter predominantly tectonically accreted muddy and sandy lithologies, including turbidites.

Site-specific objectives include the following:

- Identify the location of the primary thrust fault, including the distribution and density of fractures visible in borehole resistivity images, and any associated structure that can be inferred from bedding dips. These data will help to constrain fracture permeability and kinematic models of thrust and fold development.
- Characterize the lithologic composition and geophysical properties of the footwall and hanging wall sedimentary sequences, including their density, resistivity, porosity, NGR, sonic velocity, consolidation state, and gas hydrate content.
- Acquire downhole temperature data that will inform interpretations of future borehole observatory measurements and help to constrain the loci of thermally driven dehydration reactions and their relationship to SSE source regions.
- Identify the present maximum and minimum stress orientations from borehole breakouts. In combination with rock physical properties data, these data will be used to constrain stress magnitudes that may reflect variations in absolute strength of the plate boundary fault.
- When cores are collected, as is currently planned for Expedition 375, they will provide additional information on meso- and microscale structure, lithology, porosity, permeability, density, shear strength, age, thermal conductivity, NGR, sonic velocity, and geochemical compositions of present and past pore fluid. Pore fluid analysis of samples will help to evaluate the source of fluids above and surrounding the region of SSEs, whereas geotechnical measurements undertaken on core samples will provide information on fault and host formation permeability, consolidation state, frictional properties, and strength.

### Logging while drilling

Six LWD tools were deployed on the BHA (NeoScope, SonicScope, TeleScope, proVISION, geoVISION, and StethoScope) while drilling Holes U1518A (118 mbsf) and U1518B (600 mbsf), providing both real-time and recorded mode data to the targeted depth (Table T1). Based on the LWD physical properties measurements, six main logging units were identified and were divided into sub-units based on the observed physical properties characteristics of the sediments (Figure F12). Numerous significant features were interpreted from the logs, such as the thrust fault zone and associated sand/silt units. The fault zone, interpreted at about 320 mbsf, is associated with a reduction in resistivity and density and an increase in porosity with depth. Details of the fault location and slip distribution are expected to be derived from coring during Expedition 375. The hanging wall of the thrust fault is characterized by high  $V_p$  and  $V_s$ , and the footwall is characterized by relatively low velocity. A high-amplitude seismic reflection interval in the footwall sequence is associated with interpreted sandy sediments characterized by increased borehole washout beneath 350 mbsf. Within this interval, an abrupt change in physical properties occurs close to 370 mbsf, where a deeper fault possibly occurs. Clusters of both resistive and conductive fractures were observed in the resistivity images, more commonly in the fault hanging wall sequence. Borehole breakouts

can be observed toward the base of the hole. The StethoScope tool was deployed six times at two stations; however, none of the pore pressure measurements were successful because the tool was unable to make a seal with the borehole wall.

### Log-seismic integration

Site U1518 LWD measurements were integrated with seismic Line 05CM04 (Figure F12), which crosses the site at common depth point (CDP) 4319. Five seismic units (SUs), defined from reflection characteristics, were correlated with logging units through a time-depth relationship derived from the high-quality sonic  $V_p$  data. Of particular interest, the ~70 m thick highly reflective SU 3 (300–370 mbsf) encompasses the major thrust and the rock units in the hanging wall and footwall directly adjacent to the fault zone. The strong reflections in this SU are likely caused by the large impedance variations among the lithostratigraphic units, the possible fluid-rich interval, and the units with increased bed thickness and coarser sediments.

### Site U1519

Site U1519 (proposed Site HSM-01A) is located on the upper continental slope approximately 35 km from shore (Figure F2). The site is located on regional seismic Profile 05CM-04 at the landward edge of a 12 km wide mid-slope sedimentary basin at 1000 m water depth (Figures F2, F5). The basin is officially unnamed but is referred to here as the North Tuaheni Basin. The slope west of the basin rises to the edge of the continental shelf and hosts the North Tuaheni Landslide. This landslide and other landslides immediately to the north that are geomorphically more juvenile delivered late Quaternary MTDs directly into the basin. The seafloor in the basin is underlain by these deposits and is approximately horizontal, with localized relief of <20 m in the area of the drilling site.

Active thrust faults of the upper plate reach the seafloor on the shelf west of Site U1519 and on the mid–lower slope to the south-east. No active thrust faults are recognized directly beneath the North Tuaheni Basin; however, an apparently inactive northwest-dipping thrust lies 1.1 km below Site U1519 (Figure F3). This fault is associated with a northwest-dipping eroded hanging wall sequence. The plate interface thrust characterized by SSEs lies about 5 km below the basin floor.

The primary objective at Site U1519 was to acquire LWD data to 650 mbsf to help characterize the nature of the sedimentary sequences before a planned borehole observatory is installed during Expedition 375. Coring operations at Site U1519 are also planned for Expedition 375. The objective of the borehole observatory is to record measurements of pressure and temperature over multiple SSE cycles at a site on the inner margin approximately above the loci of large SSE displacements modeled from geodetic data. In addition to assisting in the planning of observatory targets, LWD logs and core from Site U1519 will provide constraints on the evolution of the upper slope and basin environment, as well as the timing of apparent thrust cessation across this section of the inner continental slope.

Site-specific objectives include the following:

- Characterize the lithologic composition and geophysical properties of the basin above the SSE source region to assist in the selection of stratigraphic targets for the borehole observatory installation. This includes characterizing the formation density, resistivity, porosity, NGR, sonic velocity, consolidation state, and gas hydrate content.

- Identify the distribution and density of fractures visible in borehole images to evaluate deformation of the basin at a subseismic scale.
- Identify the present maximum and minimum stress orientations from borehole breakouts and compare these with data from the other sites to evaluate regional variations in contemporary stress across the margin.
- When cores are collected, as is currently planned for Expedition 375, they will provide additional information on meso- and microscale structure, lithology, porosity, permeability, density, shear strength, age, thermal conductivity, NGR, sonic velocity, and geochemical compositions of present and past pore fluid. Pore fluid analysis of samples will help to evaluate the source of fluids above the region of SSEs, whereas geotechnical measurements undertaken on core samples will provide information on formation permeability, consolidation state, frictional properties, and strength.

### Logging while drilling

Hole U1519A was logged to the target depth of 650 mbsf. Six LWD tools were deployed on the BHA (NeoScope, SonicScope, TeleScope, proVISION, geoVISION, and StethoScope) while drilling Hole U1519A, providing both real-time and recorded mode data. Based on the LWD measurements, three main logging units and ten subunits were identified (Figure F13). From 140 to 220 mbsf, significant low values of gamma ray, resistivity, and velocity due to washout of the borehole are associated with an inferred increase in sand content. Other similar intervals are recognized near 300 and 450 mbsf. Below 550 mbsf, resistive layers are well identified in the imaged interval. The intervals are characterized by the spikes of high resistivity (tens of ohm meters) and velocity. Borehole breakouts are identified in the interval from 597 to 650 mbsf. Bedding features show various direction and angles throughout the borehole. The fractures occur sparsely throughout the borehole and include a notable high-density cluster just below the sandy interval (around 230 mbsf).

### Log-seismic integration

LWD logs were correlated to a depth-converted version of seismic Line 05CM-04 and high-resolution seismic Line TAN1404-P3106 (Figure F13). The quality of the LWD data was sufficient for correlation, except for some gaps in compressional velocity and missing density at the top of the site. The three main logging units were tied to the boundaries of the three seismic stratigraphic units. In particular, the image data matches very well with the amplitudes and architecture of the reflections in the high-resolution seismic data. Mismatches in depth between the seismic and log data will allow us to refine the velocity profile at the drill site in order to better convert the depth section.

## Site U1520

Site U1520 is located on the floor of the Hikurangi Trough between the deformation front and Tūranganui Knoll (Figures F2, F10). The site lies approximately 95 km from shore and 16 km east of the deformation front at 3521 m water depth (Figure F2). The seafloor in this location is a flat plain, and in the vicinity of Site U1520, it is underlain by about 1 km of sediment overlying the inferred volcanic rocks of the Hikurangi Plateau (Figure F3). This sequence of sedimentary and volcanic rocks collectively represents the inputs to the subduction zone. The cover sedimentary sequence in this area is condensed relative to the southern Hikurangi margin,

where up to 9 km of the total sedimentary section, including 6 km of Miocene to recent turbidites, overlies the plateau.

Regional bathymetric data show that the Tūranganui Knoll is one of numerous seamounts that characterize the northern Hikurangi Plateau. Predrilling interpretations of regional seismic reflection lines and gravity anomaly data indicate irregular crustal relief also beneath the Hikurangi Trough, with seamounts and ridges of various scales buried beneath the sedimentary sections to varying degrees. At the deformation front west of Site U1520, practically the entire sedimentary cover sequence is accreting, with the plate interface décollement located close to the top of the plateau volcanics.

The primary objective at Site U1520 was to acquire LWD data to 1200 mbsf to constrain the accreting sequence and upper part of the subducting volcanic section. This site represents the first ever drilling in the Hikurangi Trough. Through correlation of the sequences away from the drilling site to the deformation front on seismic sections, it was expected that the LWD data would provide insight into the lithologies and conditions at the shallow part of the subduction plate interface where SSEs are believed to occur close the trench. The site was intentionally located adjacent to Tūranganui Knoll, where the turbidite trench section is relatively condensed compared to farther west, closer to the deformation front. In addition to LWD data acquired during Expedition 372, coring at the site is also planned for Expedition 375.

Based on predrilling interpretation of the Hikurangi Trough seismic data, consideration of regional Hikurangi Plateau seismic stratigraphy, and previous drilling at Ocean Drilling Program Site 1124 (Leg 181) on the eastern side of the plateau, the sequence at Site U1520 was expected to include the following:

- About 610–640 m of clastic sediments, including turbidites, MTDs, hemipelagic sediments, and volcanic ash, all likely to be Pliocene–Quaternary in age. This sequence includes the Ruatoria avalanche MTD.
- About 210–230 m of predominantly pelagic sedimentary sequence of Late Cretaceous (?) to Miocene age. This interval may include nannofossil chalk, mudstone, tephra, and unconformities.
- The top of the volcanic rocks of the Hikurangi Plateau at about 840 mbsf.
- Basalts and volcanoclastic rocks, including breccia, chert, and/or limestone rocks, immediately below 840 mbsf.

Site-specific objectives include the following:

- Characterize the lithologic composition and geophysical properties, such as formation density, resistivity, porosity, NGR, and sonic velocity, of the Hikurangi Trough inputs sequence “protolith” to provide insights into possible interplate thrust fault zone and host rock properties.
- Identify the distribution and density of fractures visible in borehole images to evaluate deformation and stress state of the input section east of the deformation front at subseismic scale.
- Identify the present maximum and minimum stress orientations from borehole breakouts and compare these with data from the other sites to evaluate regional variations in contemporary stress across the margin.
- When cores are collected, as is currently planned for Expedition 375, they will provide additional information on lithology, porosity, permeability, density, meso- and microscale structure, shear strength, age, thermal conductivity, NGR, sonic velocity, and geochemical compositions of present and past pore fluid

and information on the sediment source and depositional process. Pore fluid analysis of samples will help to evaluate the source of fluids, whereas geotechnical measurements undertaken on core samples will provide information on fault zone protolith host formation permeability, consolidation state, frictional properties, and strength. The combined LWD and core data from all input sites will enable refined depth conversion of the existing 2-D and planned 3-D seismic data. They will also extend knowledge of in situ conditions (stress, fault zone properties, and pore pressure) away from the boreholes over a much broader region.

Overall, these objectives will constrain (1) the composition and frictional properties of subduction inputs and the shallow plate interface, (2) the hydrologic and thermal conditions of the incoming plate and shallow fault, and (3) the structural character, stress conditions, and mechanical properties of the main active thrust and subduction inputs.

### Logging while drilling

Time constraints due to downtime during Expedition 372 meant that drilling to the target depth of 1200 mbsf was not achievable. The site was drilled to a total depth of 750 mbsf. Six LWD tools (NeoScope, SonicScope, TeleScope, proVISION, geVISION, and StethoScope) were deployed in Holes U1520A and U1520B, providing both real-time and recorded mode data (Table T1). In both holes, the resistivity image quality suffers from slip and stick as a result of the high drilling penetration rate.

References to major reflection units determined from seismic sections were used to help define logging units relevant to the stratigraphic architecture of the sedimentary section in the Hikurangi Trough. Nine logging units were identified in Hole U1520B, reflecting significant changes in the sediment physical properties recorded by the logs (Figure F14). The uppermost 100 m is interpreted to be relatively sandy sediment, mainly turbidities, associated with borehole washouts. These overlie approximately 110 m of finer grained sediments of the Ruatoria MTD. The sediments beneath the Ruatoria MTD comprise alternating fine- and coarser grained sedimentary packages that show progressive compaction associated with increasing density and decreasing porosity with depth to a boundary at around 510 mbsf. At this depth there is a marked change to sediments that have a different acoustic character, higher density, and significantly lower gamma ray. Several further units with distinct logging characteristics are identified in the lower 150 m of the borehole. Although the logs do not enable direct identification of the rock type, the petrophysical characteristics and the tie to seismic reflectivity indicate that the pelagic sequence overlying the Tūrangānui Knoll was partially drilled. Owing to generally poor hole conditions and a fast rate of penetration, the image logs are poor quality through much of the drilled section in both Holes U1520A and U1520B. Dipping beds, however, were identified in many of the logging units. Above approximately 510 mbsf, bedding dip inclination and azimuth appear to be variable, particularly in the Ruatoria MTD. In the underlying sequence, the bedding dips are most commonly at low angles to the northwest, west, and southwest. Several high-angle resistive fractures were identified in the sediments between 100 and 150 mbsf and between 660 and 710 mbsf in Hole U1520B.

### Log-seismic integration

The seismic data available for Site U1520 allows correlation with the LWD data from Holes U1520A and U1520B (Figure F14). Seven seismic stratigraphic units were defined based on the reflection geometry and amplitude patterns. Several of the unit interfaces correspond to either erosion by landslides or unconformities. At this site, there is a very good correlation between the LWD logging units and the seismic stratigraphic units, with density, gamma ray, and resistivity curves showing pronounced shifts in their curve trends at depths concordant with seismic unit boundaries. The upper 406 mbsf is generally characterized by relatively low seismic amplitudes. The upper 102 mbsf is characterized by strong reflections, whereas the underlying Ruatoria MTD stands out as a 126 m thick package composed of chaotic, mottled, and weaker reflections. The sequences below 406 mbsf are characterized by markedly higher amplitudes associated with inferred sandy (turbidite) deposits that dip gently northwest. The lower part of Hole U1520B coincides with an increasing occurrence of irregular high-amplitude seismic reflections. The basin-filling strata generally onlaps a low-amplitude package with chaotic reflections located along the flank of the Tūrangānui Knoll. Prominent changes in density, porosity, and gamma ray occur at about 630 mbsf, close to the expected transition from hemipelagic basin fill to pelagic sediments. Synthetic seismograms produced from the density and velocity logs generally show good correlations with the seismic data analyzed.

## Preliminary scientific assessment

Expedition 372 combined two research topics, SSEs on subduction faults (IODP Proposal 781A-Full) and actively deforming gas hydrate-bearing landslides (Proposal 841-APL). Our study area on the Hikurangi margin east of New Zealand provided a unique location for addressing both research topics within the same area of continental margin.

### Hikurangi subduction slow slip

The northern HSM, New Zealand, offered us a globally unique opportunity to use ocean floor drilling technology within IODP to study SSEs on a subduction thrust fault. SSEs at northern Hikurangi are among the best-documented from land-based and offshore geodetic monitoring and are the shallowest known SSEs on Earth. They recur about every 2 years and appear to extend close to the trench, where clastic and pelagic sediments about 1.0–1.5 km thick overlie the subducting Hikurangi Plateau. These attributes made the northern Hikurangi margin amenable to an ambitious scientific drilling program involving LWD, coring, and installation of borehole observatories. To achieve this program, IODP scheduled this work across two expeditions on the *JOIDES Resolution* (Expeditions 372 and 375; Saffer et al., 2017). Drilling during Expedition 372 represented the first IODP scientific drilling ever targeted at SSE phenomena.

The overall goal of Expeditions 372 and 375 collectively is to acquire data that will help determine the physical processes associated with SSEs on subduction megathrusts and identify the factors that lead to slow slip occurring on some faults, whereas others faults or parts of the same remain interseismically strongly coupled. The strategy devised across the two expeditions was to acquire LWD data and cores from two sites above the slow slipping plate boundary and up to two sites on the subducting Hikurangi Plateau. The



former sites will have observatories installed to monitor pressure, temperature, and fluid flow transients expected through the upper plate in association with SSE cycles. The eastern Hikurangi Trough and Hikurangi Plateau sites target sequences that are either subducting or accreting at the deformation front and may host the slow slipping interplate thrust at shallow depths. These sequences are referred to as the subduction inputs. Drilling and coring the complete sediment package in the Hikurangi Trough is aimed at providing insights into the geological, geophysical, and mechanical properties of the décollement host rocks further west and down-dip. Laboratory-based geotechnical experiments on samples to be collected during Expedition 375 will furthermore reveal frictional and strength properties of rocks thought to lie in the SSE source region of the interplate thrust.

Three sites were targeted for LWD during Expedition 372, the first phase of the Hikurangi subduction program:

- Site U1519 in an upper margin slope basin in which an observatory installation is planned for Expedition 375;
- Site U1518 into one of the frontal thrusts at the toe of the accretionary wedge, up-dip of the SSE source region, and a target for the second observatory installation during Expedition 375; and
- Site U1520 in the Hikurangi Trough about 15 km east of the deformation front.

A range of LWD tools were successfully deployed at the subduction sites during Expedition 372. These included the geoVISION, providing electrical imaging; the NeoScope, providing propagation resistivity and neutron porosity; the SonicScope, providing compressional, shear, and Stoneley wave slowness; the Telescope, providing measurement-while-drilling data; and the proVISION Plus, for NMR. The LWD data were collected to (1) monitor in real time for gas entering the borehole or formation overpressures, (2) help identify targets for in situ pressure measurements, (3) facilitate lithologic interpretation, (4) guide interpretation of faults and fractures, (5) determine the maximum and minimum stress directions, (6) estimate hydrate saturation, (7) help constrain elastic moduli for integration with seismic data, and (8) provide guidance for observatories to be installed during Expedition 375. Another downhole measurement plan for Expedition 372 included using the StethoScope tool to determine formation pressure. This tool uses a probe inserted into the formation wall at selected depths and has never been deployed by IODP, although a similar wireline measurement was made using the Modular Formation Dynamics Tester during Integrated Ocean Drilling Program Expedition 319 (Expedition 319 Scientists, 2010). During Expedition 372, the StethoScope was deployed at Site U1518 six times at two stations but failed to record pressure measurements due to a lack of mud seal at the borehole wall.

Overall, the drilling depths achieved at the three subduction sites were reasonably successful considering Expedition 372 suffered time constraints due to two bad weather events that passed through the region and to operational delays departing Australia related to biosecurity requirements in New Zealand waters. Target drilling depths were reached at both Sites U1518 (600 mbsf) and U1519 (650 mbsf; Table T1). At Site U1520 in the Hikurangi Trough, we achieved 750 mbsf of the total planned depth of 1200 mbsf as a result of advised operational rescheduling to complete other aspects of the expedition.

Some general drilling highlights are outlined below for each site.

#### **Site U1518: frontal accretionary wedge thrust fault**

The primary objective at Site U1518 during Expedition 372 was to log to 600 mbsf through one of the primary thrust faults that emerge from the plate interface in the SSE source region. The goal was to acquire LWD data to help characterize the structure and location of the shallow part of the fault and the nature of the sedimentary sequences that host it. These data will be integrated with proposed cores from this site planned for Expedition 375, and both types of data will be used to identify suitable formations and fault rock for hosting a borehole observatory planned for installation during Expedition 375.

We drilled two holes (U1518A and U1518B) because bad weather interrupted Hole U1518A. Hole U1518B produced excellent quality logging data and exciting on board science. We successfully drilled to the target depth of 600 mbsf and infer that we penetrated the thrust fault zone at about 320 mbsf. This depth is very close to that predicted from various depth-converted seismic reflection data made available to us prior to drilling. Not unexpectedly, the logs reveal a sequence above the fault with different physical properties than those below the fault (Figure F12), partly resulting from inferred relatively older material being thrust over relatively younger material. In addition, changes in seismic reflection character within the drilled interval, thought to be related to lithology during predrilling interpretation of seismic data, produced closely aligned changes in logging parameters with depth. The logging data reveal detailed insights into the likely lithologies in the borehole and physical properties that will enable advanced analyses of deformation, bedding attitude, thrust mechanics, stress state, and hydrogeology. We successfully identified the distribution and density of fractures visible in borehole images and associated structures that can be inferred from bedding dips. These data will help to constrain fracture permeability and kinematic models of thrust and fold development. We also observed borehole breakouts that will allow us to identify the present maximum and minimum stress orientations. Another important success at Site U1518 is the geophysical resolution provided by the logging data, which will be valuable to assist in selecting depth targets for the borehole observatory installation planned for Expedition 375.

#### **Site U1519: upper margin slope basin**

The primary objective at Site U1519 was to log to 650 mbsf to help characterize the nature of the sedimentary sequences before a planned borehole observatory installation during Expedition 375. We successfully acquired generally good quality logging data to the target depth. We found an excellent correlation between changes in logging parameters and three major sedimentary sequences that were interpreted on seismic reflection profiles prior to drilling (Figure F13). In addition, a remarkably good match occurs between subunits recognized in the logs and complex subunits that were inferred to correspond to changes in lithology in the seismic data. Shipboard analysis indicates that the logs provide information on bedding thicknesses and dips, fracture orientations, and density. The lower part of the borehole successfully penetrated a west-dipping sedimentary sequence beneath the seafloor that lies on the landward (back limb) side of an apparently inactive thrust fault. Borehole breakouts in the lower part of the hole will provide indications of current stress directions, whereas logging properties, such as compressional and shear wave velocity and density data, will improve analysis of seismic reflection data away from the borehole site.

As with Site U1518, an important success at Site U1519 is the geophysical resolution that is provided by the logging data, which will assist in planning the bore observatory installation during Expedition 375.

#### **Site U1520: Hikurangi Trough, subduction inputs sequence**

The primary objective at Site U1520 was to acquire LWD data to 1200 mbsf to constrain the accreting sequence and upper part of the subducting volcanic section. This site represents the first ever drilling in the Hikurangi Trough. Through correlation of the sequences away from the site to the deformation front on seismic sections, it was expected that the LWD data would provide insight into the lithologies and conditions at the subduction plate interface where SSEs are believed to occur close the trench.

We drilled two holes (U1520A and U1520B) because bad weather interrupted Hole U1520A (Table T1). Hole U1520B reached a total depth of 750 mbsf and was then abandoned to undertake other work at Site U1517. Consequently, we did not reach our predrilling objective of drilling through the oldest sedimentary sequences and penetrating the inferred volcanic rocks corresponding to the lower flank of Tūrangānui Knoll. Acquisition of LWD data to 750 mbsf, however, will provide Expedition 375 with operational flexibility when returning to the site for coring. Coring operations planned for Expedition 375 at this site and possibly at proposed Site HSM-08A (Saffer et al., 2017) will be critical to achieve the outcomes of the combined science program.

Because the turn-around time for shore-based processing of LWD data was typically about three days and this site was drilled close to the end of the expedition, our shipboard interpretations for this site are based on some unprocessed LWD data.

The LWD logs at this site reveal numerous changes in physical properties downhole that match very well against depth-converted seismic reflection data (Figure F14). As at the other sites, we found that changes in borehole conditions revealed by the ultrasonic caliper and other logging properties, such as density, resistivity, porosity, and gamma ray, coincide well with changes in seismic reflection amplitudes and packages of seismic stratigraphy. In the upper and mid-reaches of the borehole, we drilled through sequences we infer to be predominantly turbidites and the distal reaches of the Ruatoria MTD. Although the shipboard data are preliminary, based on drilling depths and logging signatures, and consideration of the seismic sections, we believe we drilled beneath the base of the Hikurangi Trough clastic sequence and into the inferred pelagic cover sequence of the Hikurangi Plateau.

### **Tuaheni Landslide Complex**

The primary drilling goal for the TLC was to understand the mechanisms behind the slow deformation of the landslides and their proposed links to gas hydrates by logging and sampling through the landslide mass and the gas hydrate stability zone. To achieve this goal, we planned to obtain lithologic information within the creeping slides, collect samples for shore-based laboratory studies, constrain in situ gas hydrate saturation and composition, analyze pore water profiles, obtain pore pressure and temperature profiles, study fracturing, and calibrate seismic data from our study area.

Operationally, we originally planned to conduct LWD surveys at three sites, the main Site U1517 in the extensional, creeping part of the TLC, a site in the compressional part of the TLC above the BGHS pinch-out (proposed Site TLC-02C), and a reference site outside the slide mass (planned primary Site TLC-03B). We planned to

core Site U1517 with the APC/HLAPC system and deploy the T2P/SETP to measure pore pressure and temperature and the pressure core sampler (PCS) to collect sediment cores under pressure for calibration of gas hydrate saturation and for gas hydrate composition. This plan allowed a comprehensive study of the creeping part of the TLC and comparison with both its compressional part and gas hydrates in the vicinity but outside the slide mass. Because of significant downtime, we focused all our operations on the main site (U1517), conducting LWD, coring, and a reduced number of T2P/SETP stations, skipping the other two sites. This compromise aimed to minimize the impact of reduced operational time on addressing our scientific goals.

#### **Meeting the objectives of the expedition: Tuaheni Landslide Complex**

We consider the TLC program overall successful in terms of allowing us to test our hypotheses and antitheses despite the significant downtime we experienced. Importantly, we were able to complete almost the entire planned program at the main site (U1517). We were not, however, able to log either a site in the compressional part of the slides (proposed Site TLC-02C) or a reference site outside the slide mass (proposed Site TLC-03B). Results from gas hydrate occurrences in the deeper preslide mass interval at Site U1517, combined with the detection of gas hydrates at Site U1519, should allow us to interpret results from Site U1517 without a reference site. Extension of results from Site U1517 based on recently acquired long-offset 2-D seismic data should also alleviate the lack of LWD in the compressional part of the slide. Although we were fortunate to still be able to successfully deploy the T2P and SETP within a very limited time window, we could not deploy the PCS. The objectives of pressure coring were to constrain gas hydrate saturation and composition. We are confident that we were able to get accurate and continuous profiles of gas hydrate saturation because of the high quality of the LWD data. A number of chloride measurements provide independent and robust saturation measurements in the 10 cm range. Pressure cores would have yielded average saturations over 1 m, closer to the resolution of LWD data and thus better suited for calibration. We may be able to improve calibration of LWD data using planned laboratory experiments. We are confident we will obtain sufficient information on gas composition in hydrates from the recovered hydrate samples.

We have largely achieved the scientific objectives, listed below:

- TLC Objective 1: obtain lithologic information within the creeping slides, in particular across the proposed décollement of creeping. We had >90% core recovery with the only major gaps occurring below the BGHS, probably due to gas expansion.
- TLC Objective 2: collect samples for shore-based laboratory studies. This objective relates to gas hydrate studies: 13 whole rounds that, based on infrared images, are likely to contain gas hydrates were stored in liquid nitrogen and will be shipped for laboratory studies to the GeoForschungsZentrum Potsdam (Germany), the Qingdao Institute of Marine Geology (China), and the British Geological Survey. Additional whole rounds and other samples of gas hydrate-free sediment were collected for laboratory studies involving gas hydrate formation followed by geomechanical measurements.
- TLC Objective 3: constrain in situ gas hydrate saturation and composition. Because of the high quality of logs and excellent core recovery, including gas hydrate samples, we are confident this objective has been achieved for Site U1517. Proposed LWD Site TLC-02C in the compressional part of the slides is outside

the hydrate stability zone, and thus hydrates are not expected to be present there. We do not have available any LWD-based gas hydrate saturation from a reference site outside the slide mass (proposed Site TLC-03B). However, we are confident we have sufficient information from Site U1519 and from the preslide interval at Site U1517 to not require the reference site for future evaluation.

- TLC Objective 4: obtain pore pressure and temperature profiles. This objective was aimed at Site U1517. We were able to measure the temperature gradient above the BGHS. We successfully measured formation pressure at a critical depth near the base of the landslide debris. At the time of writing, we have not been able to retrieve data from a second deployment because of issues with the data logger—we are hopeful we will be able to recover the data. Given the novel design of the T2P probe, we consider this deployment a significant success.
- TLC Objective 5: search for evidence of fracturing. Resistivity images from LWD will allow us to detect fracturing at Site U1517. Although we will not be able to compare fracture patterns with those in the compressional region of the slides, we may still be able to gain some information on changes in any fracture patterns from the seismic data.
- TLC Objective 6: calibrate seismic data. The excellent logs should provide full calibration of the short-streamer 3-D seismic site survey at Site U1517. Canceling two additional wells within the 3-D cube will increase uncertainties in inversion approaches away from Site U1517, but this effect is partly alleviated by the acquisition of a long-streamer seismic line across Site U1517 by the *Marcus Langseth* in November and December 2017, which will enhance constraints away from the borehole.

In a much broader sense, the nearly full recovery of cores through the landslide and the gas hydrate zone provides us with an excellent record of sedimentology, lithology, physical properties, and geochemistry. The LWD data are high quality, providing important structural and geophysical information, as well as calibration for the various seismic data sets covering the TLC. Combined with achieving most of the objectives listed above, we are confident that postexpedition analyses will allow us to illuminate the processes leading to “creeping” of the TLC—the primary goal of Proposal 841-APL. Some highlights of our findings are summarized below.

### Gas hydrates

Gas hydrates are inferred to be present in the preslide interval from ~110 mbsf to the BGHS at ~160 mbsf based on LWD data, chlorinity profiles, and direct sampling. They appear to be absent within the landslides. Gas hydrates appear to be mostly present in thin, coarser grained layers that have hydrate saturations reaching up to 68%, based on pore water chlorinity. Gas in headspace samples consists almost entirely of methane with only small fractions of ethane in a limited depth interval. Furthermore, a number of gas hydrate occurrences can be inferred from LWD data at Sites U1518 and U1519.

### Submarine landslide processes

LWD- and laboratory-based physical properties indicate consistent variation between the landslide debris mass and underlying sediment. Disequilibrium profiles from geochemical results through the TLC reflect temporal elements of the depositional structure of the system. Core lithologies are dominated by graded fine sandy beds and clayey silts, including many turbidites. These

results, combined with core-log and seismic integration that provides petrophysical properties within the slide mass and surrounding lithologies, provide an exceptional framework for analyzing active landslide processes.

### Logging while drilling

In Hole U1517A, five LWD tools were deployed on the BHA, providing both real-time and recorded mode data through the TLC, below the décollement, and through the BSR. Based on the LWD measurements, five main logging units were identified that closely correspond to lithostratigraphic units defined for cores from Hole U1517C (Figure F11). Several significant features were interpreted from the logs, such as a compacted, low-porosity base of the debris flow from 54 to 60 mbsf and natural gas hydrate occurring in 10–30 cm thick turbidite sands from 110 to 150 mbsf. Both conductive and resistive fractures were also identified throughout the hole; however, the highest fracture density occurred within the landslide. Expedition 372 provided the rare opportunity of a comprehensive LWD program in, by industry standards, relatively shallow sediments. Subsequently, postexpedition research projects include development of LWD methodology.

## Operations

During Expedition 372 we conducted LWD, piston coring, and formation temperature and pressure operations in nine holes at four sites. A total of 2589.4 m was either drilled for LWD or advanced without recovery for selected probe measurements. A total interval of 197.9 m was cored at Site U1517, and 186.84 m of core was recovered (94% total core recovery) (Table T1). Here, we describe the operations at each of the sites. The overall time distribution for the 39 day expedition included 7.3 days in port, 14.2 days in transit, and 17.5 days on site. The vessel transited a total of 3928 nmi.

### Fremantle port call

Expedition 372 began at 0742 h (UTC + 8 h) on 26 November 2017 with the first line ashore at Victoria Quay in Fremantle, Australia. The IODP *JOIDES Resolution* Science Operator (JRSO) technical staff and chief scientists boarded the vessel at 0930 h, and the Expedition 369 science party disembarked at 1130 h. Port call activities started with IODP JRSO staff crew change and crossover. The off-going technical staff departed the vessel at 1530 h. The ship crew change and crossover occurred on 27 November. The Schlumberger LWD and measurement-while-drilling tools were loaded onto the ship along with other Schlumberger supplies and a new wireline.

To comply with the New Zealand ship biofouling regulations, the ship scheduled a 2 day hull cleaning operation at anchorage outside of Fremantle. The vessel departed Victoria Quay with the last line away at 1148 h on 1 December. After a 10 nmi transit, the ship arrived at anchorage at 1311 h. The hull cleaning barge arrived at around 1400 h and commenced work immediately.

Hull cleaning concluded at 1610 h on 3 December, and the pilot came aboard the vessel at 1652 h. After pulling up the anchor at 1706 h, the vessel began the sea passage to Site U1517 at 1830 h.

### Transit to Site U1517

After a 3419 nmi transit, the ship arrived at Site U1517 at 0200 h (UTC + 13 h) on 16 December 2017. The voyage took 291.9 h (12.2 days) at an average of 11.7 kt.



## Site U1517

Site U1517 consisted of four holes ranging in depth from 9.4 to 205.0 mbsf. Operations at Site U1517 included LWD, piston coring, and formation pressure and temperature measurements. In total, 37 cores were recorded for Site U1517.

LWD operations with continuous safety monitoring advanced to 205 mbsf in Hole U1517A. A total of 186.84 m of core over a 197.9 m interval was recovered from Holes U1517B and U1517C using the APC and HLAPC systems (94% core recovery). Hole U1517D was drilled to 168.7 mbsf with probe deployments at four locations. The total time spent on site at Site U1517 was 5.1 days.

### Hole U1517A

Once the vessel arrived on site the thrusters were lowered, and the ship moved to the site coordinates at 0247 h on 16 December 2017. The APC/extended core barrel (XCB) BHA was put together in preparation for Hole U1517B. The LWD tool string was assembled and contained the geoVISION, SonicScope, NeoScope, TeleScope, and proVISION tools. The entire LWD BHA was 190.72 m in length.

The precision depth recorder (PDR) placed the seafloor at 722.5 meters below sea level (mbsl), and the BHA was lowered to 672 mbsl for flow and pressure testing of the LWD tools to determine the flow rates at which the tools activate. The subsea video camera was deployed to observe the drill bit tag the seafloor, which occurred at 1755 h. The seafloor depth for Hole U1517A was 725.4 mbsl. The camera system was retrieved, and drilling in Hole U1517A commenced at 1935 h on 16 December. The bit advanced at an average rate of 20 m/h. LWD in Hole U1517A continued through 17 December, reaching the total depth of 205 mbsf at 1115 h. After a 30-barrel mud sweep, the drill pipe and LWD BHA were pulled from the hole with the logging tools continuing to record sonic measurements. The bit cleared the seafloor at 1245 h and the rotary table at 1840 h on 17 December, ending Hole U1517A.

### Hole U1517B

The vessel was offset 20 m southeast (heading of 155°) for coring operations in Hole U1517B. The APC/XCB BHA was assembled and run to 704 mbsl. The bit was spaced out, and the first core was shot at 720 mbsl. Hole U1517B began at 0130 h on 18 December 2017, and Core 1H recovered 9.4 m of sediment. The mudline in this core could not be identified with certainty. The decision was made to abandon Hole U1517B and attempt to recover a mudline core at the same hole location.

### Hole U1517C

The bit was raised 4 m, and coring in Hole U1517C began at 0210 h on 18 December 2017. APC Cores 1H and 2H were drilled to 15.2 mbsf before switching to the HLAPC to recover a silt-rich interval. Cores 3F through 14F (15.2–71.6 mbsf) were taken before switching back to the APC for Cores 15H through 18H (71.6–108.3 mbsf), all of which had partial strokes and were advanced by recovery. The HLAPC was redeployed for Cores 19F through 36F (108.3–188.5 mbsf). Of these, Cores 19F, 20F, 22F, 23F, 25F through 28F, and 30F through 36F all recorded partial strokes and were advanced by recovery, with the exception of Cores 34F through 36F, which were advanced by 4.7 m. All of the APC cores were oriented using either the FlexIT tool (Cores 1H and 2H) or the Icefield MI-5 core orientation tool (Cores 15H through 18H). The APCT-3 was run on Cores 15H, 17H, 20F, 23F, 26F, 29F, and 34F. A total of 177.44 m of core was recovered from the 188.5 m interval (94%). Six APC cores

were taken over a 51.9 m interval with 52.66 m recovered (101%). Thirty HLAPC cores were taken over a total interval of 136.6 m with 124.78 m recovered (91%).

After reaching the total depth of 188.5 mbsf, the drill pipe was pulled out of the hole and the bit cleared the seafloor at 1015 h on 19 December and the rotary table at 1220 h, ending Hole U1517C. The ship was secured for the 20 nmi transit to Site U1518 at 1310 h on 19 December.

### Hole U1517D

The vessel returned to Site U1517 at 2300 h on 31 December 2017 following a 32 nmi transit from Site U1520. The BHA was made up, and the drill string was assembled in preparation for formation temperature and pressure measurements. Hole U1517D began at 0720 h on 1 January 2018 and was drilled to 80 mbsf. The center bit was retrieved, and the motion decoupled hydraulic delivery system (MDHDS) and T2P probe were deployed to make measurements of in situ formation pressure and temperature. The shear pins failed to shear on the first attempt, and a second attempt was made ~1 h later. This time, the shear pins sheared and the T2P was inserted into the sediment. The tool could not be recovered using the Electronic Release System (ERS) on the Schlumberger wireline and had to be picked up using the coring winch. Upon retrieval, it was noted that the T2P probe tip was damaged, having lost the thermistor in the tip; however, it did record a good pressure measurement. The center bit was installed, and the hole was drilled to 120 mbsf. After the center bit was retrieved, a second T2P probe was deployed. After sitting in the formation for ~45 min, the ERS, again could not retrieve the tool, and the core winch was used. Upon recovery to the rig floor, it was noted that the second T2P was also damaged upon recovery, this time missing the entire tapered probe tip, and the electronics had been flooded. This damage likely occurred during tool recovery. The hole was drilled to 130 mbsf, and the sediment temperature pressure tool (SETP) was successfully deployed using the colleted delivery system. The hole was drilled to a total depth of 168.7 mbsf, and a final SETP measurement was made. The drill string was pulled from the hole and the bit cleared the seafloor at 1030 h and the rotary table at 1315 h. The ship was secured for transit, and Site U1517 ended at 1536 h on 2 January when the ship began the transit to Lyttelton, New Zealand.

## Site U1518

Site U1518 consisted of two LWD holes that were drilled to 117.8 and 600 mbsf (Table T1). Continuous LWD safety monitoring was performed during operations at both holes. The total operational time at Site U1518 was 3.4 days with 21 h of that time spent waiting on weather.

### Hole U1518A

The vessel arrived at Site U1518 at 1635 h (UTC + 13 h) on 19 December 2017 after a 20 nmi transit from Site U1517. The LWD BHA and drill pipe were run to 300 mbsl, and the LWD tools were flow tested. After the test, drill string assembly continued. The LWD tool string for Site U1518 contained the geoVISION, NeoScope, StethoScope, TeleScope, SonicScope, and proVISION tools.

The LWD tools and drill string were run to 2460 mbsl, and the subsea camera was deployed to determine the depth of the seafloor. While the camera descended, 115 ft of drill line was cut off. The seafloor was tagged at 2636.4 mbsl. The camera was brought to the surface, and the top drive was installed. Hole U1518A began at 0855 h on 20 December. Weather conditions and sea state deteriorated

over the next few hours, and the logging tools were pulled out of the hole at 1605 h, ending Hole U1518A. LWD data was collected from 0 to 117.8 mbsf. The ship began waiting on weather and was offset 20 m southeast of Hole U1518A.

#### Hole U1518B

At 1310 h on 21 December 2017, an attempt was made to begin Hole U1518B; however, sea conditions were still too rough and prevented the start of the hole. After an additional 3 h of waiting on weather, Hole U1518B successfully began at 1600 h. In total, 21 h was spent waiting on weather. LWD operations continued to 372.7 mbsf. After logging a portion of the inferred thrust fault zone, the tools were pulled up to 334.7 mbsf. Three pore pressure measurements were attempted using the StethoScope tool, and all failed to provide formation pressure measurements. The tools were then pulled up to 234.0 mbsf to try three additional StethoScope measurements, which were unsuccessful as well. The tools were lowered back to the bottom of the hole, a mud sweep was used to clean the hole, and the tools advanced to 372.7 mbsf. LWD continued to a total depth of 600 mbsf. After finishing the hole, a 30-barrel mud sweep was used to clean out the hole. The LWD tools and drill string were pulled out of the hole with the bit clearing the seafloor at 1825 h on 23 December. The ship was secured for transit at 0257 h on 24 December, ending Site U1518. The seafloor depth for Hole U1518B was 2634.6 mbsl based on the LWD logs.

#### Site U1519

The ship arrived at Site U1519 at 0530 h (UTC + 13 h) on 24 December 2017 after a 15.4 nmi transit from Site U1518. The LWD BHA was assembled and contained the geoVISION, NeoScope, StethoScope, TeleScope, SonicScope, and proVISION tools. The LWD tools and drill string were deployed to 952 mbsl, and the tools were tested before starting the hole. Hole U1519A began at 1200 h on 24 December and continued to 26 December. LWD safety monitoring proceeded during all LWD operations. After logging to 650 mbsf, a 30-barrel mud sweep was used to clean the hole. The LWD tools and drill string were pulled out of the hole and the bit cleared the seafloor at 0425 h and the rotary table at 0855 h. The ship began the transit to Site U1520 at 0910 h on 26 December, ending Site U1519. The seafloor depth for Hole U1519A was 1000.7 mbsl based on the LWD logs.

#### Site U1520

Site U1520 consisted of two LWD holes that were drilled to 97.9 and 750 mbsf (Table T1). The total time spent at Site U1520 was 2.9 days, with 45.75 h of that time waiting on weather. LWD safety monitoring was employed while operating in both holes.

#### Hole U1520A

The vessel arrived at Site U1520 at 1302 h (UTC + 13 h) on 26 December 2017. The 210.30 m long LWD BHA was assembled, including the geoVISION, NeoScope, StethoScope, TeleScope, SonicScope, and proVISION tools. The BHA was deployed to 390 mbsl and flow tested to determine the appropriate flow rates. The proVISION tool was not sending real-time data, and the drill string was recovered so that the spare proVISION tool could be deployed. The tools and drill string were set at 390 mbsl for a second LWD tool test. Again, the proVISION tool failed to send real-time information. The tool string was deployed to the seafloor (3527.4 mbsl), and Hole U1520A began at 0845 h on 27 December. The proVISION began sending real-time data once the tool was turned on. The

weather and sea conditions began to deteriorate, and the drill string had to be pulled out of Hole U1520A after reaching 97.9 mbsf. Hole U1520A ended when the bit cleared the seafloor at 1410 h on 27 December. Based on the LWD data, the seafloor depth for Hole U1520A was 3521.3 mbsl.

#### Hole U1520B

The vessel waited on the weather to clear for 45.75 h (1.91 days). During this time, the ship was offset 20 m northwest of Hole U1520A at a bearing of 300°. Hole U1520B began at 1245 h on 29 December. The seafloor depth was 3520.1 mbsl based on the LWD data. The hole was washed down to 80 mbsf, and LWD measurements were taken from 80 to 750 mbsf. After reaching the total depth of 750 mbsf at 0430 h on 31 December, the hole was cleaned with a 30-barrel mud sweep and the drill string was pulled out of the hole. The bit cleared the seafloor at 0715 h and the rotary table at 1930 h. The LWD tools were broken down, and the vessel began the 32 nmi transit to Site U1517 at 1954 h, ending Site U1520.

### Transit to Lyttelton

The 404 nmi transit to Lyttelton, New Zealand began at 1536 h (UTC + 13 h) on 2 January 2018 after completing operations in Hole U1517D.

The vessel reached the pilot station at 0600 h on 4 January 2018, and Expedition 372 ended with the first line ashore at 0706 h in Lyttelton, New Zealand.

## Education and outreach

Expedition 372 had two Education and Outreach Officers from the United States and New Zealand who communicated the scientific operations and objectives with audiences of all ages around the world. The educators conducted a series of live ship-to-shore broadcasts with classrooms, meetings, offices, workshops, and families throughout the duration of the expedition. Additionally, the Outreach Officers produced online content highlighting aspects of ship life; ship operations; science goals; Science, Technology, Engineering, and Mathematics (STEM) career paths; and other careers at sea in the form of blog posts, YouTube videos, and social media content (Twitter, Facebook, and Instagram).

### Webcasts

Using iPads and the Zoom video conferencing software, the Education and Outreach Team conducted 35 live broadcasts with shore-based groups that lasted 30–70 min. During these broadcasts, the educators provided an introduction to the *JOIDES Resolution* and Expedition 372 science objectives; presented a tour of the forecastle, core, and bridge decks; and arranged for the students to ask questions of *JOIDES Resolution* technicians and expedition scientists. Over the course of the expedition, these live broadcasts reached a total of approximately 1460 people in 6 countries. Audiences included school-aged children from Years 2 (age = 6–7) through 13 (age = 17–18), university classes, and public events with groups of scientists and the general public.

In advance of broadcasts with classrooms, the Outreach Officers provided the teachers with educational materials about the *JOIDES Resolution* and Expedition 372. The officers also coordinated with the teachers regarding broadcast content to ensure it fit within the educational content and goals for each classroom. Topics included ocean-related and sea-going careers, STEM careers, expedition objectives and science, basic marine geology concepts, site-



specific tectonics and geology, natural hazards, and expedition motivations and impacts. After the broadcasts, the Education and Outreach Team received numerous thank you emails and social media posts (through Twitter and Facebook).

Because Expedition 372 spanned major world holidays, the Outreach Officers hosted a series of broadcasts geared toward friends and family members of shipboard technicians, crew, and science party members. Through these broadcasts, expedition participants had the opportunity to show their friends and family around the ship and talk about the science objectives and shift duties. Additionally, the Outreach Officers helped facilitate live broadcasts for science party members with the media and with professional workshops.

## Social media

The Education and Outreach Team maintained an expedition blog (<http://joidesresolution.org/expedition/372>), Facebook page (@joidesresolution), Twitter feed (@TheJR), YouTube channel (<https://www.youtube.com/user/theJOIDESResolution>), and Instagram account (@JOIDES\_resolution) throughout the expedition to communicate events and activities occurring on the *JOIDES Resolution* on a daily basis. The Outreach Officers produced a total of 45 blog posts, including 3 guest blogs written by science party members. Through the *JOIDES Resolution* Facebook account, the Outreach Officer created over 60 posts, and the number of followers increased by 1%–2% during the expedition. A total of 52 Expedition 372 Twitter posts and retweets were made with an average of approximately 1,550 impressions, 66 engagements, 4 retweets, and 13 likes per tweet. Furthermore, approximately 80 new Twitter followers were added. A total of 24 videos were uploaded to the *JOIDES Resolution* YouTube channel and were cross-promoted across other social media platforms. A total of 15 posts were also made on the *JOIDES Resolution* Instagram account, garnering dozens of new followers.

## Media

The Education and Outreach Officers helped facilitate communication between science party members and various media outlets. This effort included helping to set up interviews for print media in Ireland and New Zealand, audio interviews for a Futureproof podcast in Ireland, and a video creation for the Irish Times. An event for the New Zealand media was also held on the final day of the expedition at the Lyttelton, New Zealand, port call. The Co-Chief Scientists summarized the preliminary results from the expedition, media interviews were conducted, and members of the media were given tours of the ship.

## Postexpedition projects

Both Outreach Officers will continue their educational activities on shore with several planned projects. One project involves producing a mini online course for teachers and students with five modules related to the Expedition 372 and 375 scientific objectives. The modules will focus on New Zealand tectonics, marine geology, and geomorphology and cover the following topics: plate tectonics with a New Zealand focus, subduction zone dynamics, submarine landslides and tsunami hazards, gas hydrates, and SSEs/shallow sea-floor structure. These models are being created in consultation with the Expedition 375 New Zealand Outreach Officer and will be used as post-Expedition 372 and pre-Expedition 375 resources. These modules will be hosted on the *JOIDES Resolution* website under the “For Educators” page and will be linked to both the Expedition 372

and 375 web pages. Though geared toward secondary school students, the material from these modules will be easily adaptable to most any age group.

Another postexpedition project is a publication to be submitted to the peer-reviewed *Journal of Science Education and Technology*. This paper will focus on case examples of telepresence and “ship-to-shore” programs, including the education and outreach programs of the *JOIDES Resolution*, *E/V Nautilus*, and NOAA’s *Okeanos Explorer*. Specific details on the content are still being determined, but the article will generally focus on discussing the ship-to-shore and telepresence aspects of the programs, as well as the types of education and outreach work being done and their impacts on promoting STEM fields.

An ocean-related “career map” will be created to illustrate the many different potential career options in which someone can work with the ocean and/or have a sea-going career. The goal in creating this career map is to help people better understand the many different ocean-related career options that exist and to provide information on how they can achieve those careers. It is intended to be used by students or others to learn about different potential career options and the education and training they will need to achieve that career. This career map will include information from and tie together the blogs, interviews, and other activities that occurred while at sea during Expedition 372, which will also be incorporated into the final product.

A presentation is also planned for a session at the Ocean Sciences Meeting 2018 in February 2018 in Portland, Oregon. This meeting is sponsored by the Association for the Sciences of Limnology and Oceanography, American Geophysical Union, and The Oceanography Society and will feature a wide range of attendees from academia, industry, research institutions, government agencies, nongovernmental organizations, and education and outreach programs.

## References

- Alexander, C.R., Walsh, J.P., and Orpin, A.R., 2010. Modern sediment dispersal and accumulation on the outer Poverty continental margin. *Marine Geology*, 270(1–4):213–226. <https://doi.org/10.1016/j.margeo.2009.10.015>
- Audet, P., Bostock, M.G., Christensen, N.I., and Peacock, S.M., 2009. Seismic evidence for overpressured subducted oceanic crust and megathrust fault sealing. *Nature*, 457(7225):76–78. <https://doi.org/10.1038/nature07650>
- Bangs, N.L.B., and Gulick, S.P.S., 2005. Physical properties along the developing décollement in the Nankai Trough: inferences from 3-D seismic reflection data inversion and Leg 190 and 196 drilling data. In Mikada, H., Moore, G.F., Taira, A., Becker, K., Moore, J.C., and Klaus, A. (Eds.), *Proceedings of the Ocean Drilling Program, Scientific Results*, 190/196: College Station, TX (Ocean Drilling Program), 1–18. <https://doi.org/10.2973/odp.proc.sr.190196.354.2005>
- Barker, D.H.N., Sutherland, R., Henrys, S., and Bannister, S., 2009. Geometry of the Hikurangi subduction thrust and upper plate, North Island, New Zealand. *Geochemistry, Geophysics, Geosystems*, 10(2):Q02007. <https://doi.org/10.1029/2008GC002153>
- Barnes, P., and TAN 1114 Scientific Party, 2011. *NIWA Voyage Report TAN1114*: Auckland, New Zealand (National Institute of Water and Atmospheric Research). [https://www.niwa.co.nz/sites/niwa.co.nz/files/os2020\\_northern\\_hikurangi\\_margin\\_geohazards.pdf](https://www.niwa.co.nz/sites/niwa.co.nz/files/os2020_northern_hikurangi_margin_geohazards.pdf)
- Barnes, P.M., Cheung, K.C., Smits, A.P., Almagor, G., Read, S.A.L., Barker, P.R., and Froggatt, P., 1991. Geotechnical analysis of the Kidnappers slide, upper continental slope, New Zealand. *Marine Geotechnology*, 10(1–2):159–188. <https://doi.org/10.1080/10641199109379888>

- Barnes, P.M., Lamarche, G., Bialas, J., Henrys, S., Pecher, I., Netzeband, G.L., Greinert, J., Mountjoy, J.J., Pedley, K., and Crutchley, G., 2010. Tectonic and geological framework for gas hydrates and cold seeps on the Hikurangi subduction margin, New Zealand. *Marine Geology*, 272(1–4):26–48. <https://doi.org/10.1016/j.margeo.2009.03.012>
- Barnes, P.M., Nicol, A., and Harrison, T., 2002. Late Cenozoic evolution and earthquake potential of an active listric thrust complex above the Hikurangi subduction zone, New Zealand. *Geological Society of America Bulletin*, 114(11):1379–1405. [https://doi.org/10.1130/0016-7606\(2002\)114<1379:LCEAEP>2.0.CO;2](https://doi.org/10.1130/0016-7606(2002)114<1379:LCEAEP>2.0.CO;2)
- Baum, R.L., Savage, W.Z., and Wasowski, J., 2003. Mechanics of earthflows. In Picarelli, L. (Ed.), *Proceedings of the International Workshop on Occurrence and Mechanisms of Flow-Like Landslides in Natural Slopes and Earthfills*: Bologna, Italy (Associazione Geotecnica Italiana), 185–190.
- Bell, R., Sutherland, R., Barker, D.H.N., Henrys, S., Bannister, S., Wallace, L., and Beavan, J., 2010. Seismic reflection character of the Hikurangi subduction interface, New Zealand, in the region of repeated Gisborne slow slip events. *Geophysical Journal International*, 180(1):34–48. <https://doi.org/10.1111/j.1365-246X.2009.04401.x>
- Chang, C., McNeill, L.C., Moore, J.C., Lin, W., Conin, M., and Yamada, Y., 2010. In situ stress state in the Nankai accretionary wedge estimated from borehole wall failures. *Geochemistry, Geophysics, Geosystems*, 11:Q0AD04. <https://doi.org/10.1029/2010GC003261>
- Chiswell, S., 2005. Mean and variability in the Wairarapa and Hikurangi Eddies, New Zealand. *New Zealand Journal of Marine and Freshwater Research*, 39(1):121–134. <https://doi.org/10.1080/00288330.2005.9517295>
- Collot, J.-Y., Lewis, K., Lamarache, G., and Lallemand, S., 2001. The giant Ruetoria debris avalanche on the northern Hikurangi margin, New Zealand; result of oblique seamount subduction. *Journal of Geophysical Research: Solid Earth*, 106(B9):19271–19297. <https://doi.org/10.1029/2001JB900004>
- Crutchley, G.J., Geiger, S., Pecher, I.A., Gorman, A.R., Zhu, H., and Henrys, S.A., 2010. The potential influence of shallow gas and gas hydrates on sea floor erosion of Rock Garden, an uplifted ridge offshore of New Zealand. *Geo-Marine Letters*, 30(3–4):283–303. <https://doi.org/10.1007/s00367-010-0186-y>
- Davy, B., Hoernle, K., and Werner, R., 2008. Hikurangi Plateau: crustal structure, rifted formation, and Gondwana subduction history. *Geochemistry, Geophysics, Geosystems*, 9(7):Q07004. <https://doi.org/10.1029/2007GC001855>
- Durham, W.B., Kirby, S.H., Stern, L.A., and Zhang, W., 2003. The strength and rheology of methane clathrate hydrate. *Journal of Geophysical Research: Solid Earth*, 108(B4):2182. <https://doi.org/10.1029/2002JB001872>
- Ellis, S., Fagereng, A., Barker, D., Henrys, S., Saffer, D., Wallace, L., Williams, C., and Harris, R., 2015. Fluid budgets along the northern Hikurangi subduction margin, New Zealand: the effect of a subducting seamount on fluid pressure. *Geophysical Journal International*, 202(1):277–297. <https://doi.org/10.1093/gji/ggv127>
- Ellis, S., Pecher, I., Kukowski, N., Xu, W., Henrys, S., and Greinert, J., 2010. Testing proposed mechanisms for seafloor weakening at the top of gas hydrate stability on an uplifted submarine ridge (Rock Garden), New Zealand. *Marine Geology*, 272(1–4):127–140. <https://doi.org/10.1016/j.margeo.2009.10.008>
- Expedition 319 Scientists, 2010. Methods. In Saffer, D., McNeill, L., Byrne, T., Araki, E., Toczko, S., Eguchi, N., Takahashi, K., and the Expedition 319 Scientists, *Proceedings of the Integrated Ocean Drilling Program*, 319: Tokyo (Integrated Ocean Drilling Program Management International, Inc.). <https://doi.org/10.2204/iodp.proc.319.102.2010>
- Field, B.D., Uruski, C.L., Bey, A., Browne, G., Crampton, J., Funnell, R., Killops, S., Laird, M., Mazengarb, C., Morgans, H., Rait, G., Smale, D., and Strong, P., 1997. *Cretaceous–Cenozoic Geology and Petroleum Systems of the East Coast Region, New Zealand* (Volume 19): Lower Hutt, New Zealand (Institute of Geological and Nuclear Sciences).
- Ghissetti, F.C., Barnes, P.M., Ellis, S., Plaza-Faverola, A.A., and Barker, D.H.N., 2016. The last 2 Myr of accretionary wedge construction in the central Hikurangi margin (North Island, New Zealand): insights from structural modeling. *Geochemistry, Geophysics, Geosystems*, 17(7):2661–2686. <https://doi.org/10.1002/2016GC006341>
- Hensen, C., Wallmann, K., Schmidt, M., Ranero, C.R., and Suess, E., 2004. Fluid expulsion related to mud extrusion off Costa Rica—a window to the subducting slab. *Geology*, 32(3):201–204. <https://doi.org/10.1130/G20119.1>
- Huhn, K., 2016. DSRV Sonne SO247 Cruise Report—SlamZ: slide activity on the Hikurangi margin, New Zealand, Wellington–Auckland, 27 March–27 April 2016. Bundesministerium für Bildung und Forschung. [https://www.portal-forschungsschiffe.de/lw\\_resource/data-pool/items/item\\_183/fahrtbericht\\_so247.pdf](https://www.portal-forschungsschiffe.de/lw_resource/data-pool/items/item_183/fahrtbericht_so247.pdf)
- Kodaira, S., Iidaka, T., Kato, A., Park, J.-O., Iwasaki, T., and Kaneda, Y., 2004. High pore fluid pressure may cause silent slip in the Nankai Trough. *Science*, 304(5675):1295–1298. <https://doi.org/10.1126/science.1096535>
- Kopf, A., Mora, G., Deyhle, A., Frapce, S., and Hesse, R., 2003. Fluid geochemistry in the Japan Trench forearc (ODP Leg 186): a synthesis. In Suyehiro, K., Sacks, I.S., Acton, G.D., and Oda, M. (Eds.), *Proceedings of the Ocean Drilling Program, Scientific Results*, 186: College Station, TX (Ocean Drilling Program), 1–23. <https://doi.org/10.2973/odp.proc.sr.186.117.2003>
- Kvenvolden, K.A., 1993. Gas hydrates—geological perspective and global change. *Reviews of Geophysics*, 31(2):173–187. <http://dx.doi.org/10.1029/93RG00268>
- Lewis, K.B., Collot, J.-Y., and Lallemand, S.E., 1998. The dammed Hikurangi Trough: a channel-fed trench blocked by subducting seamounts and their wake avalanches (New Zealand–France GeodyNZ Project). *Basin Research*, 10(4):441–468. <https://doi.org/10.1046/j.1365-2117.1998.00080.x>
- Lin, W., Doan, M.-L., Moore, J.C., McNeill, L., Byrne, T.B., Ito, T., Saffer, D., Conin, M., Kinoshita, M., Sanada, Y., Moe, K.T., Araki, E., Tobin, H., Boutt, D., Kano, Y., Hayman, N.W., Flemings, P., Huftile, G.J., Cukur, D., Buret, C., Schleicher, A.M., Efimenko, N., Kawabata, K., Buchs, D.M., Jiang, S., Kameo, K., Horiguchi, K., Wiersberg, T., Kopf, A., Kitada, K., Eguchi, N., Toczko, S., Takahashi, K., and Kido, Y., 2010. Present-day principal horizontal stress orientations in the Kumano forearc basin of the southwest Japan subduction zone determined from IODP NanTroSEIZE drilling Site C0009. *Geophysical Research Letters*, 37(13):L13303. <https://doi.org/10.1029/2010GL043158>
- Liu, Y., and Rice, J.R., 2007. Spontaneous and triggered aseismic deformation transients in a subduction fault model. *Journal of Geophysical Research: Solid Earth*, 112(B9):B09404. <https://doi.org/10.1029/2007JB004930>
- MacMahon, J., 2016. High-resolution velocity analysis of seismic data to identify gas hydrates in the Tuaheni Landslide Complex on the Hikurangi margin, New Zealand [M.S. thesis]. University of Auckland, New Zealand.
- Martin, H.E., and Whalley, W.B., 1987. Rock glaciers. Part 1: rock glacier morphology: classification and distribution. *Progress in Physical Geography*, 11(2):260–282. <https://doi.org/10.1177/030913338701100205>
- Mienert, J., Posewang, J., and Baumann, M., 1998. Gas hydrates along the northeastern Atlantic margin: possible hydrate-bound margin instabilities and possible release of methane. In Henriot, J.-P., and Mienert, J. (Eds.), *Gas Hydrates: Relevance to World Margin Stability and Climate Change*. Geological Society Special Publication, 137(1):275–291. <https://doi.org/10.1144/GSL.SP.1998.137.01.22>
- Miyazaki, K., Yamaguchi, T., Sakamoto, Y., and Aoki, K., 2011. Time-dependent behaviors of methane-hydrate bearing sediments in triaxial compression test. *International Journal of the JCRM*, 7(1):43–48. <https://doi.org/10.11187/ijjcr.7.43>
- Mountjoy, J., Krastel, S., Crutchley, G., Dannoni, A., Graw, M., Koch, S., Micallef, A., Quinn, W., and Woelz, S., 2014a. *Niwa Voyage Report TAN1404: SCHLIP-3D: submarine clathrate hydrate landslide imaging project*: Auckland, New Zealand (National Institute of Water and Atmospheric Research).
- Mountjoy, J.J., and Barnes, P., 2011. Active upper plate thrust faulting in regions of low plate interface coupling, repeated slow slip events, and coastal uplift: example from the Hikurangi margin, New Zealand. *Geo-*

- chemistry, *Geophysics, Geosystems*, 12(1):Q01005.  
<https://doi.org/10.1029/2010GC003326>
- Mountjoy, J.J., Krastel, S., Gross, F., and Pecher, I., 2016. Large creeping landslides controlled by gas hydrates? Rheological control or cyclic gas flux from the base of hydrate stability [paper presented at Gordon Research Conference, Galveston, Texas, 28 February–4 March 2016].
- Mountjoy, J.J., McKean, J., Barnes, P.M., and Pettinga, J.R., 2009. Terrestrial-style slow-moving earthflow kinematics in a submarine landslide complex. *Marine Geology*, 267(3–4):114–127.  
<https://doi.org/10.1016/j.margeo.2009.09.007>
- Mountjoy, J.J., Pecher, I., Henrys, S., Crutchley, G., Barnes, P.M., and Plaza-Faverola, A., 2014b. Shallow methane hydrate system controls ongoing, downslope sediment transport in a low-velocity active submarine landslide complex, Hikurangi Margin, New Zealand. *Geochemistry, Geophysics, Geosystems*, 15(11):4137–4156.  
<https://doi.org/10.1002/2014GC005379>
- Mulder, T., and Cochonat, P., 1996. Classification of offshore mass movements. *Journal of Sedimentary Research*, 66(1):43–57.  
<https://doi.org/10.1306/D42682AC-2B26-11D7-8648000102C1865D>
- Peacock, S.M., 2009. Thermal and metamorphic environment of subduction zone episodic tremor and slip. *Journal of Geophysical Research: Solid Earth*, 114(B8):B00A07. <https://doi.org/10.1029/2008JB005978>
- Pecher, I.A., Henrys, S.A., Ellis, S., Chiswell, S.M., and Kukowski, N., 2005. Erosion of the seafloor at the top of the gas hydrate stability zone on the Hikurangi margin, New Zealand. *Geophysical Research Letters*, 32(24):L24603. <https://doi.org/10.1029/2005GL024687>
- Pecher, I.A., Henrys, S.A., Ellis, S., Crutchley, G., Fohrmann, M., Gorman, A.R., Greinert, J., Chiswell, S.M., TAN0607 Scientific Party, and SO191 Scientific Party, 2008. Erosion of seafloor ridges at the top of the gas hydrate stability zone, Hikurangi margin, New Zealand—new insights from research cruises between 2005 and 2007 [paper presented at the 6th International Conference on Gas Hydrates, Vancouver, Canada, 6–10 July 2008]. <https://open.library.ubc.ca/cIRcle/collections/59278/items/1.0041097>
- Pedley, K.L., Barnes, P.M., Pettinga, J.R., and Lewis, K.B., 2010. Seafloor structural geomorphic evolution of the accretionary frontal wedge in response to seamount subduction, Poverty Indentation, New Zealand. *Marine Geology*, 270(1–4):119–138.  
<https://doi.org/10.1016/j.margeo.2009.11.006>
- Peng, Z., and Gombert, J., 2010. An integrated perspective of the continuum between earthquakes and slow-slip phenomena. *Nature Geoscience*, 3(9):599–607. <https://doi.org/10.1038/ngeo940>
- Phrampus, B.J., and Hornbach, M.J., 2012. Recent changes to the Gulf Stream causing widespread gas hydrate destabilization. *Nature*, 490(7421):527–530. <https://doi.org/10.1038/nature11528>
- Posamentier, H.W., and Vail, P.R., 1988. Eustatic controls on clastic deposition II—sequence and systems tract models. In Wilgus, C.K., Hastings, B.S., Posamentier, H., Van Wagoner, J., Ross, C.A., and Kendall, C.G.St.C. (Eds.), *Sea-Level Changes: An Integrated Approach*. Special Publication - SEPM (Society of Sedimentary Geologists), 42:125–154.  
<https://doi.org/10.2110/pec.88.01.0125>
- Priest, J.A., Best, A.I., and Clayton, C.R.I., 2005. A laboratory investigation into the seismic velocities of methane gas hydrate-bearing sand. *Journal of Geophysical Research: Solid Earth*, 110(B4):B04102.  
<https://doi.org/10.1029/2004JB003259>
- Ranero, C.R., Grevemeyer, I., Sahling, U., Barckhausen, U., Hensen, C., Wallmann, K., Weinrebe, W., Vannucchi, P., von Huene, R., and McIntosh, K., 2008. Hydrogeological system of erosional convergent margins and its influence on tectonics and interplate seismogenesis. *Geochemistry, Geophysics, Geosystems*, 9(3):Q03S04.  
<https://doi.org/10.1029/2007GC001679>
- Rubinstein, J.L., Shelly, D.R., and Ellsworth, W.L., 2010. Non-volcanic tremor: a window into the roots of fault zones. In Cloetingh, S., and Negendank, J. (Eds.), *New Frontiers in Integrated Solid Earth Sciences*: Dordrecht, The Netherlands (Springer), 287–314.  
[https://doi.org/10.1007/978-90-481-2737-5\\_8](https://doi.org/10.1007/978-90-481-2737-5_8)
- Saffer, D., Wallace, L., and Petronotis, K., 2017. *Expedition 375 Scientific Prospectus: Hikurangi Subduction Margin Coring and Observatories*. International Ocean Discovery Program.  
<https://doi.org/10.14379/iodp.sp.375.2017>
- Saffer, D.M., Underwood, M.B., and McKiernan, A.W., 2008. Evaluation of factors controlling smectite transformation and fluid production in subduction zones: application to the Nankai Trough. *Island Arc*, 17(2):208–230. <https://doi.org/10.1111/j.1440-1738.2008.00614.x>
- Schwartz, S.Y., and Rokosky, J.M., 2007. Slow slip events and seismic tremor at circum-Pacific subduction zones. *Reviews of Geophysics*, 45(3):RG3004.  
<https://doi.org/10.1029/2006RG000208>
- Screaton, E., Kimura, G., Curewitz, D., Moore, G., Chester, F., Fabbri, O., Ferrusson, C., Girault, F., Goldsby, D., Harris, R., Inagaki, F., Jiang, T., Kitamura, Y., Knuth, M., Li, C.-F., Claesson Liljedahl, L., Louis, L., Milliken, K., Nicholson, U., Riedinger, N., Sakaguchi, A., Solomon, E., Strasser, M., Su, X., Tsutsumi, A., Yamaguchi, A., Ujiej, K., and Zhao, X., 2009. Interactions between deformation and fluids in the frontal thrust region of the NanTroSEIZE transect offshore the Kii Peninsula, Japan: results from IODP Expedition 316 Sites C0006 and C0007. *Geochemistry, Geophysics, Geosystems*, 10(12):Q0AD01. <https://doi.org/10.1029/2009GC002713>
- Solheim, A., Berg, K., Forsberg, C.F., and Bryn, P., 2005. The Storegga Slide complex: repetitive large scale sliding with similar cause and development. In Solheim, A., Bryn, P., Berg, K., and Mienert, J. (Eds.), *Ormen Lange—an Integrated Study for the Safe Development of a Deep-Water Gas Field within the Storegga Slide Complex, NE Atlantic Continental Margin*. Marine and Petroleum Geology, 22(1–2):97–107.  
<https://doi.org/10.1016/j.marpetgeo.2004.10.013>
- Song, T.-R.A., Helmlinger, D.V., Brudzinski, M.R., Clayton, R.W., Davis, P., Pérez-Campos, X., and Singh, S.K., 2009. Subducting slab ultra-slow velocity layer coincident with silent earthquakes in southern Mexico. *Science*, 324(5926):502–506. <https://doi.org/10.1126/science.1167595>
- Tobin, H.J., and Saffer, D.M., 2009. Elevated fluid pressure and extreme mechanical weakness of a plate boundary thrust, Nankai Trough subduction zone. *Geology*, 37(8):679–682.  
<https://doi.org/10.1130/G25752A.1>
- Underwood, M.B., Saito, S., Kubo, Y., and the Expedition 322 Scientists, 2010. Expedition 322 summary. In Saito, S., Underwood, M.B., Kubo, Y., and the Expedition 322 Scientists, *Proceedings of the Integrated Ocean Drilling Program*, 322: Tokyo (Integrated Ocean Drilling Program Management International, Inc.). <https://doi.org/10.2204/iodp.proc.322.101.2010>
- Van Wagoner, J.C., Posamentier, H.W., Mitchum, R.M., Jr., Vail, P.R., Sarg, J.F., Loutit, T.S., and Hardenbol, J., 1988. An overview of the fundamentals of sequence stratigraphy and key definitions. In Wilgus, C.K., Hastings, B.S., Ross, C.A., Posamentier, H.W., Van Wagoner, J., and Kendall, C.G.St.C. (Eds.), *Sea-Level Changes: An Integrated Approach*. Special Publication - SEPM (Society of Economic Paleontologists and Mineralogists), 42:39–45.
- Wallace, L.M., and Beavan, J., 2010. Diverse slow slip behavior at the Hikurangi subduction margin, New Zealand. *Journal of Geophysical Research: Solid Earth*, 115(B12):B12402. <https://doi.org/10.1029/2010JB007717>
- Wallace, L.M., Beavan, J., McCaffrey, R., and Darby, D., 2004. Subduction zone coupling and tectonic block rotations in the North Island, New Zealand. *Journal of Geophysical Research: Solid Earth*, 109(B12):B12406.  
<https://doi.org/10.1029/2004JB003241>
- Wallace, L.M., Webb, S.C., Ito, Y., Mochizuki, K., Hino, R., Henrys, S., Schwartz, S.Y., and Sheehan, A.F., 2016. Slow slip near the trench at the Hikurangi subduction zone, New Zealand. *Science*, 352(6286):701–704.  
<https://doi.org/10.1126/science.aaf2349>
- Wech, A.G., and Creager, K.C., 2011. A continuum of stress, strength and slip in the Cascadia subduction zone. *Nature Geoscience*, 4(9):624–628.  
<https://doi.org/10.1038/ngeo1215>
- Wild, J.J., 2016. Seismic velocities beneath creeping gas hydrates slides: analysis of ocean bottom seismometer data in the Tuaheni Landslide Complex on the Hikurangi margin, New Zealand [M.S. thesis]. University of Auckland, New Zealand.
- Winters, W.J., Pecher, I.A., Waite, W.F., and Mason, D.H., 2004. Physical properties and rock physics models of sediment containing natural and labora-

tory-formed methane gas hydrate. *American Mineralogist*, 89(8–9):1221–1227. <https://doi.org/10.2138/am-2004-8-909>  
Zoback, M.D., Hickman, S., and Ellsworth, W., 2007. The role of fault zone drilling. In Kanamori, H., and Schubert, G. (Eds.), *Treatise on Geophysics*

(Volume 4); *Earthquake Seismology*: Amsterdam (Elsevier), 649–674.  
<https://doi.org/10.1016/B978-044452748-6/00084-5>

Table T1. Expedition 372 hole summary. mbrf = meters below rig floor. NA = not applicable.

Hole	Latitude	Longitude	Seafloor depth (mbrf)	Cores (N)	Cored (m)	Recovered (m)	Recovery (%)	Drilled (m)	Total penetration (m)	Total depth (mbrf)	Time on hole (h)	Time on hole (days)
U1517A	38°49.7722'S	178°28.5574'E	736.2	0	0.0	0.00	NA	205.0	205.0	941.2	40.25	1.7
U1517B	38°49.7820'S	178°28.5633'E	731.1	1	9.4	9.40	100	0.0	9.4	740.5	7.25	0.3
U1517C	38°49.7820'S	178°28.5633'E	731.8	36	188.5	177.44	94	0.0	188.5	920.3	35.50	1.5
U1517D	38°49.7765'S	178°28.5604'E	731.8	0	0.0	0.00	NA	168.7	168.7	900.5	40.00	1.7
Site U1517 totals:				37	197.9	186.84	94	373.7	571.6	NA	123.00	5.1
U1518A	38°51.5368'S	178°53.7606'E	2647.3	0	0.0	0.00	NA	117.8	117.8	2765.1	23.50	1
U1518B	38°51.5476'S	178°53.7621'E	2645.5	0	0.0	0.00	NA	600.0	600.0	3247.3	59.00	2.5
Site U1518 totals:				0	0.0	0.00	NA	717.8	717.8	NA	82.50	3.5
U1519A	38°43.6372'S	178°36.8537'E	1011.6	0	0.0	0.00	NA	650.0	650.0	1661.6	52.00	2.2
Site U1519 totals:				0	0.0	0.00	NA	650.0	650.0	NA	52.00	2.2
U1520A	38°58.1641'S	179°07.9357'E	3532.2	0	0.0	0.00	NA	97.9	97.9	3630.1	15.25	0.6
U1520B	38°58.1587'S	179°07.9233'E	3531.0	0	0.0	0.00	NA	750.0	750.0	4281.0	55.25	2.3
Site U1520 totals:				0	0.0	0.00	NA	847.9	847.9	NA	70.50	2.9
Expedition 372 totals:				37	197.9	186.84	94	2589.4	2787.3	NA	328.00	13.7



Figure F1. Tectonic setting of Expedition 372 study area (red square).

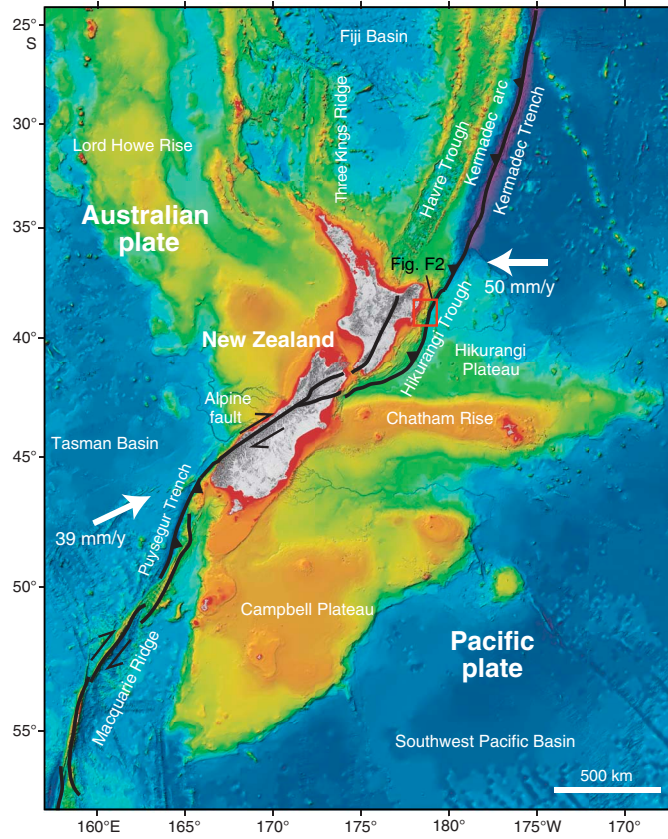


Figure F2. Bathymetry, drill site locations, and regional seismic sections, Expedition 372. Thick lines = high fold (long streamer), thin lines = low fold. Small rectangle around Site U1517 shows location of predrilling P-Cable 3-D seismic reflection data.

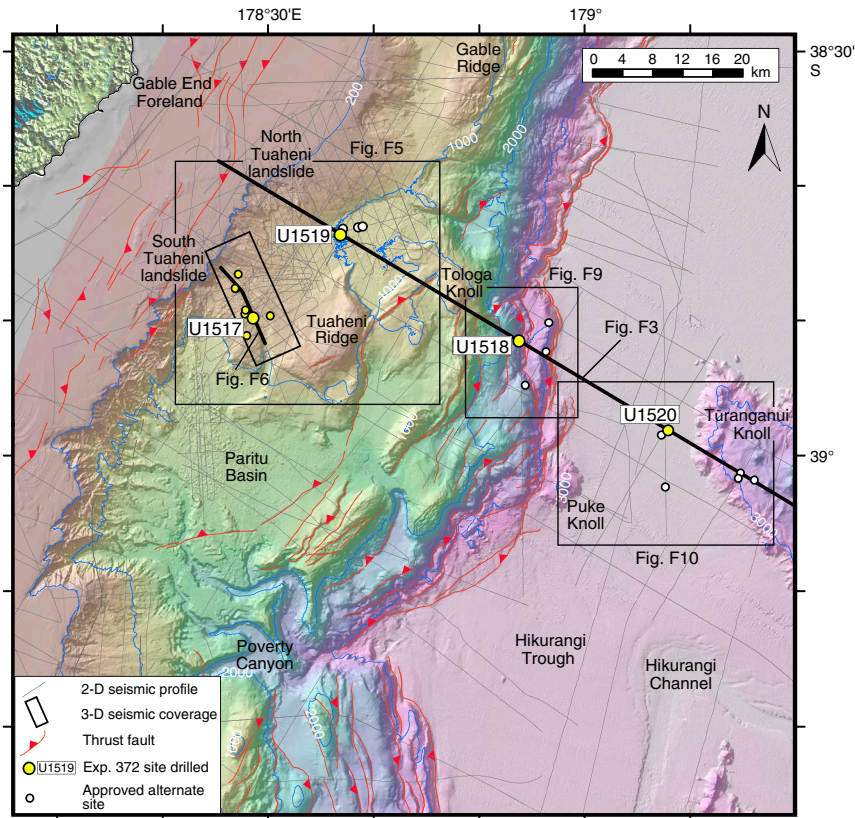


Figure F3. Interpretation of regional depth-converted seismic Profile 05CM-04 showing major faults and HSM site locations. HKB = Hikurangi Basement Sequence. Seismic depth section was provided by GNS Science, New Zealand. VE = vertical exaggeration.

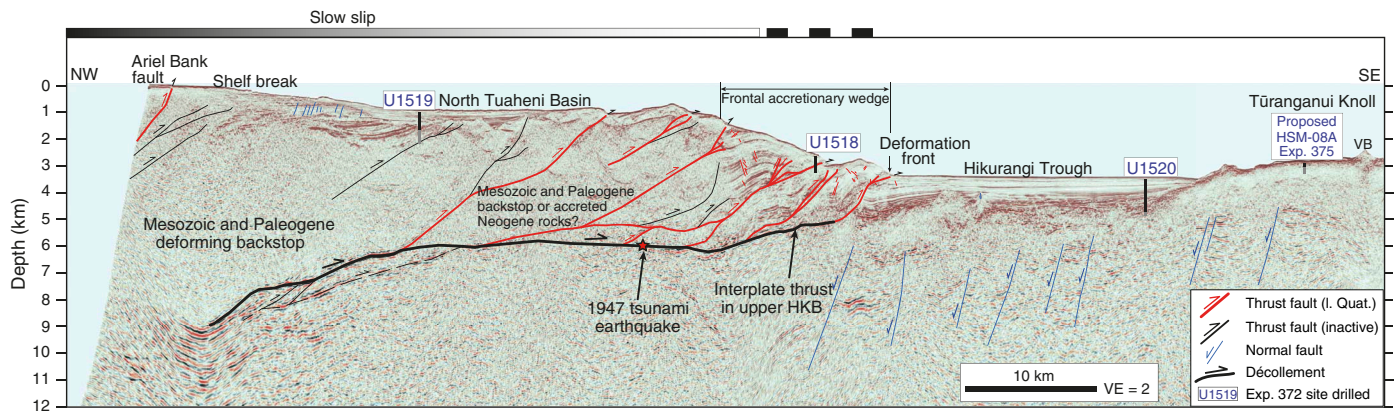


Figure F4. Regional map showing the extent of recent offshore SSEs identified by Wallace et al. (2016) using offshore geodetic data. Colored symbols = onshore cGPS stations, small circles = microearthquakes, fine red lines = major faults from Pedley et al. (2010) and Mountjoy and Barnes (2011). Inset shows example of GPS time series from near Gisborne township.

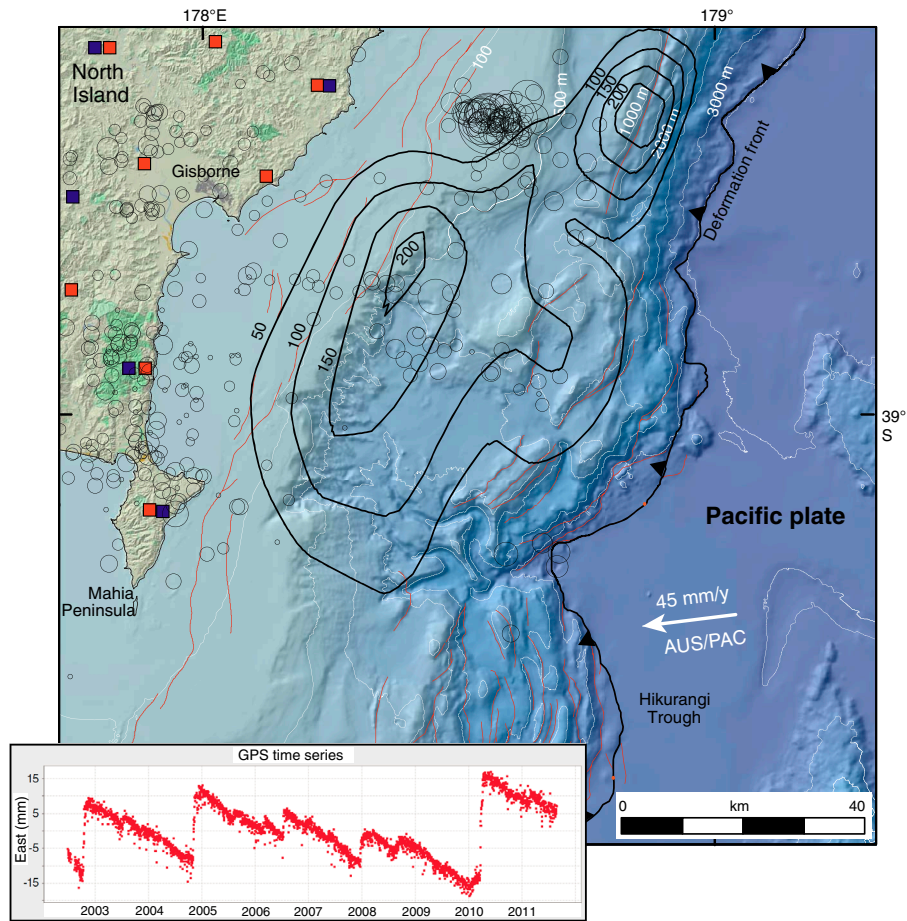




Figure F5. Bathymetry, drill site locations, and regional seismic sections on upper margin. See Figure F2 for location. Thick lines = high fold (long streamer), thin lines = low fold. Rectangle around Site U1517 shows location of predrilling P-Cable 3-D seismic reflection data.

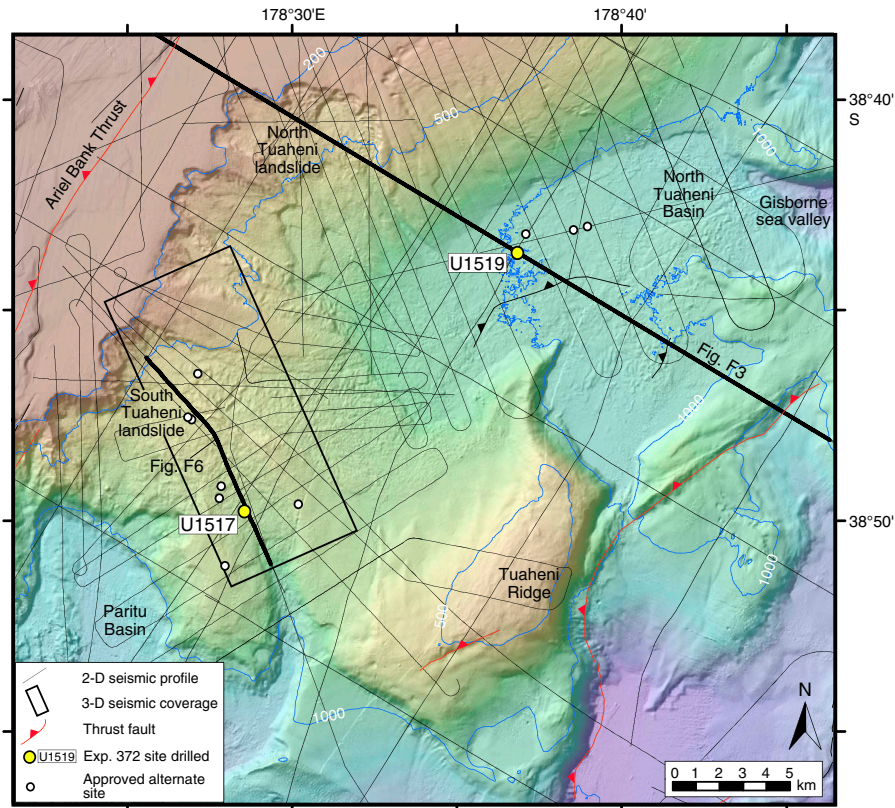


Figure F6. 2-D seismic Section TAN1114-10b across the TLC. Sites are projected onto the line. Solid line = base of TLC slide mass, dashed line = earlier interpretation of base of creeping (after Mountjoy et al., 2014b).

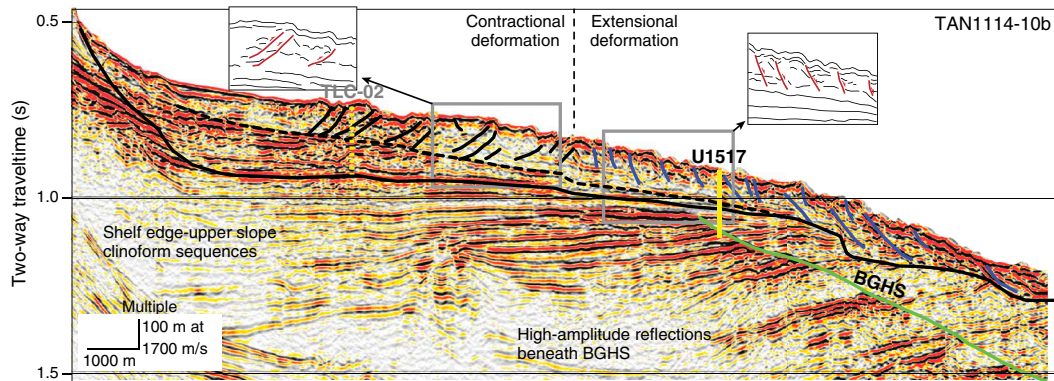


Figure F7. Hypotheses for gas hydrate-related creeping and predicted resulting sediment microstructure (after Mountjoy et al., 2014b).

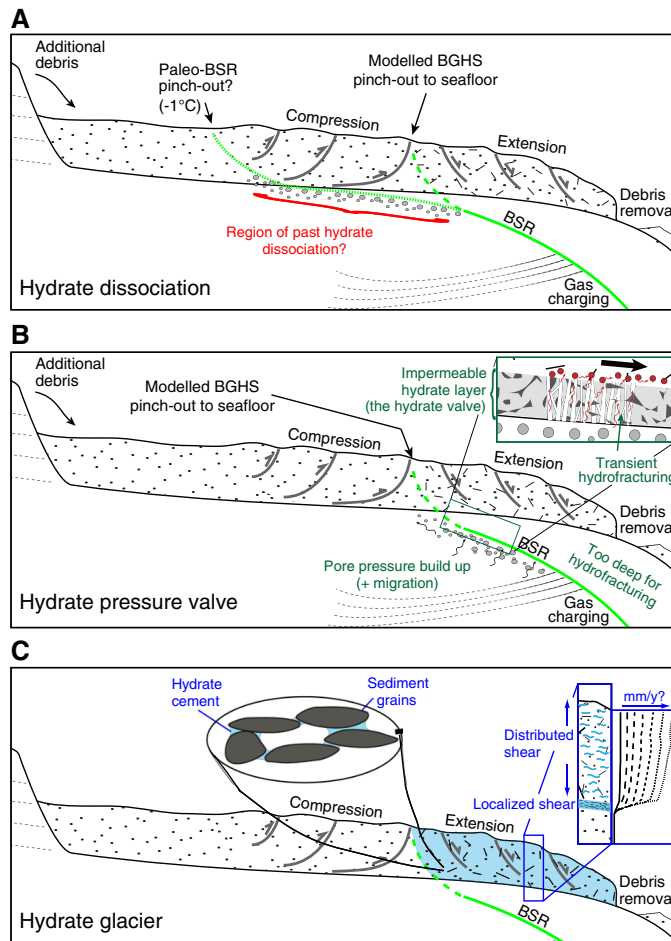


Figure F8. In-line 1778 across Site U1517 with predrilling interpretation.

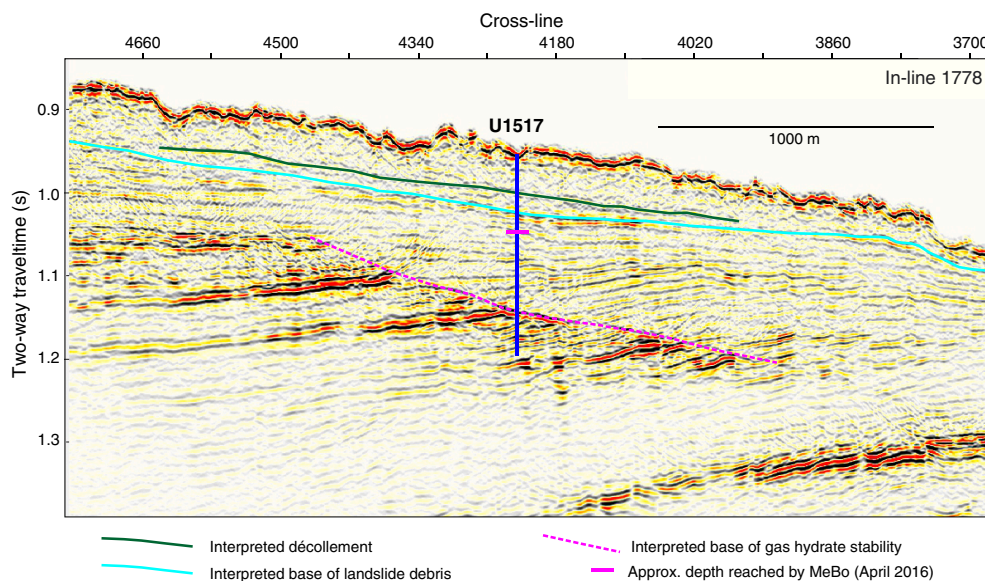




Figure F9. Bathymetry, drill site locations, and regional seismic sections on central margin. See Figure F2 for location. Thick lines = high fold (long streamer), thin lines = low fold.

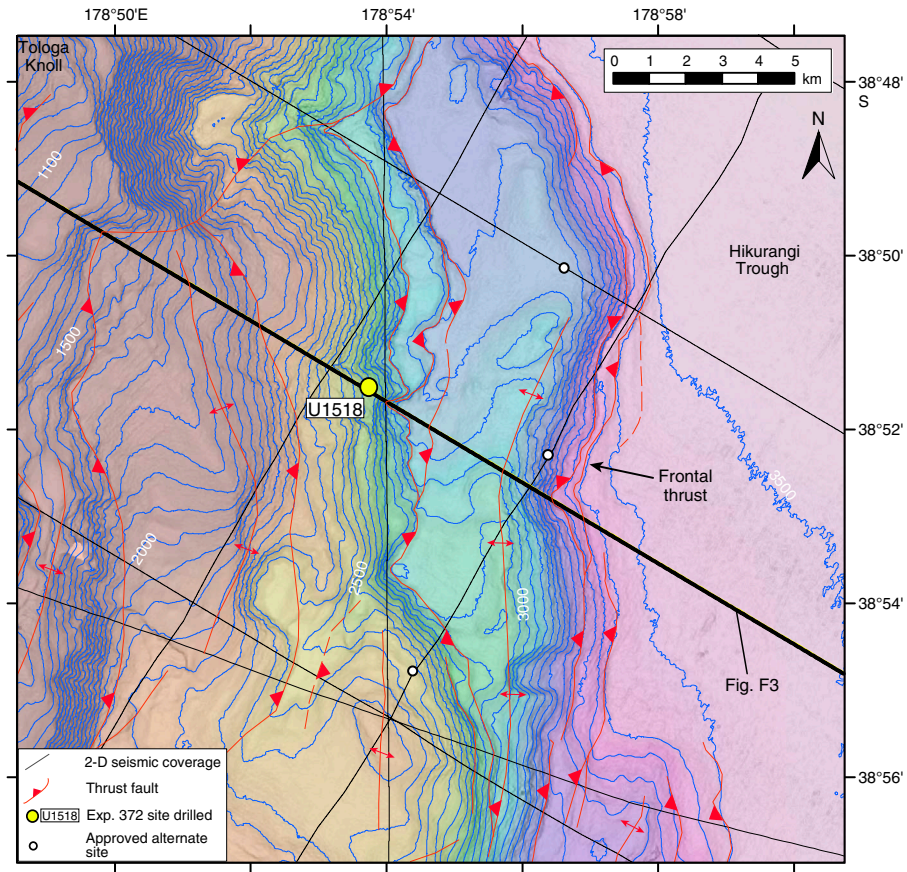


Figure F10. Bathymetry, drill site locations, and regional seismic sections on lower margin. See Figure F2 for location. Thick lines = high fold (long streamer), thin lines = low fold.

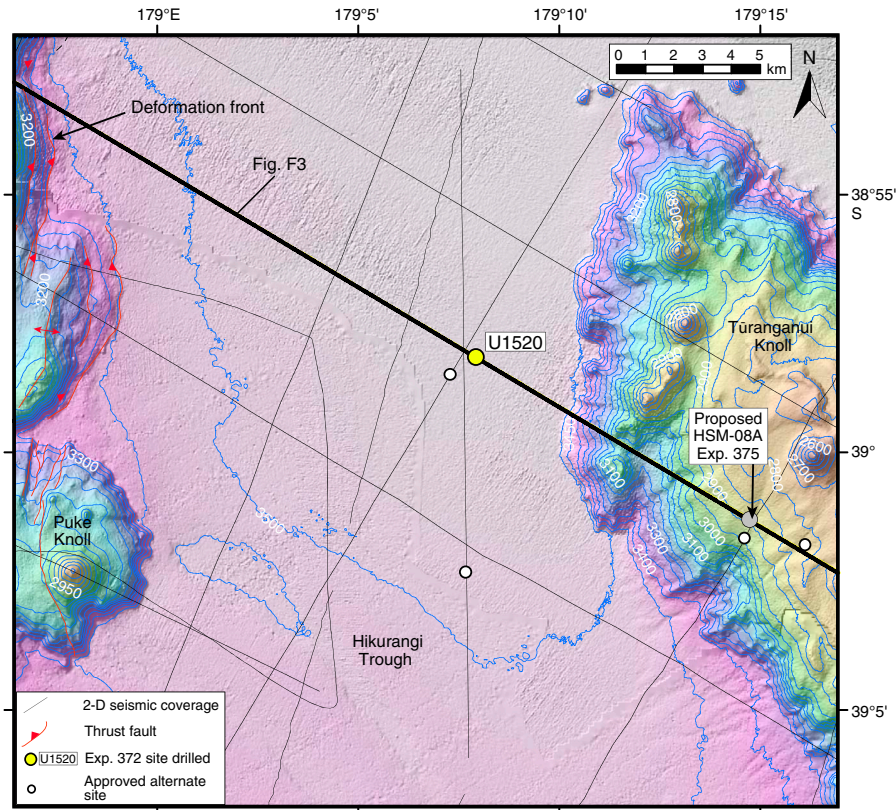


Figure F11. Composite plot of seismic image (In-line 1778) and selected measurements from LWD and cores, Site U1517. NGR = natural gamma radiation, MAD = moisture and density, NMR = nuclear magnetic resonance.

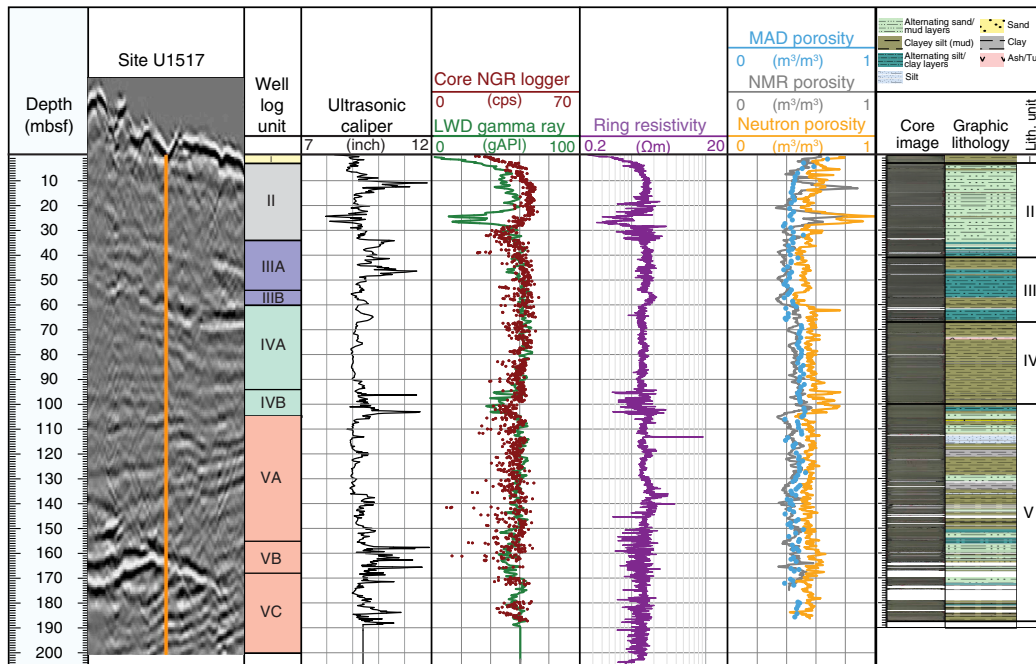


Figure F12. Composite plot of seismic image (Profile 05CM-04) and selected measurements from LWD for 50–600 mbsf, Hole U1518B. Prestack depth migration (PSDM) seismic section was provided by GNS Science, New Zealand.

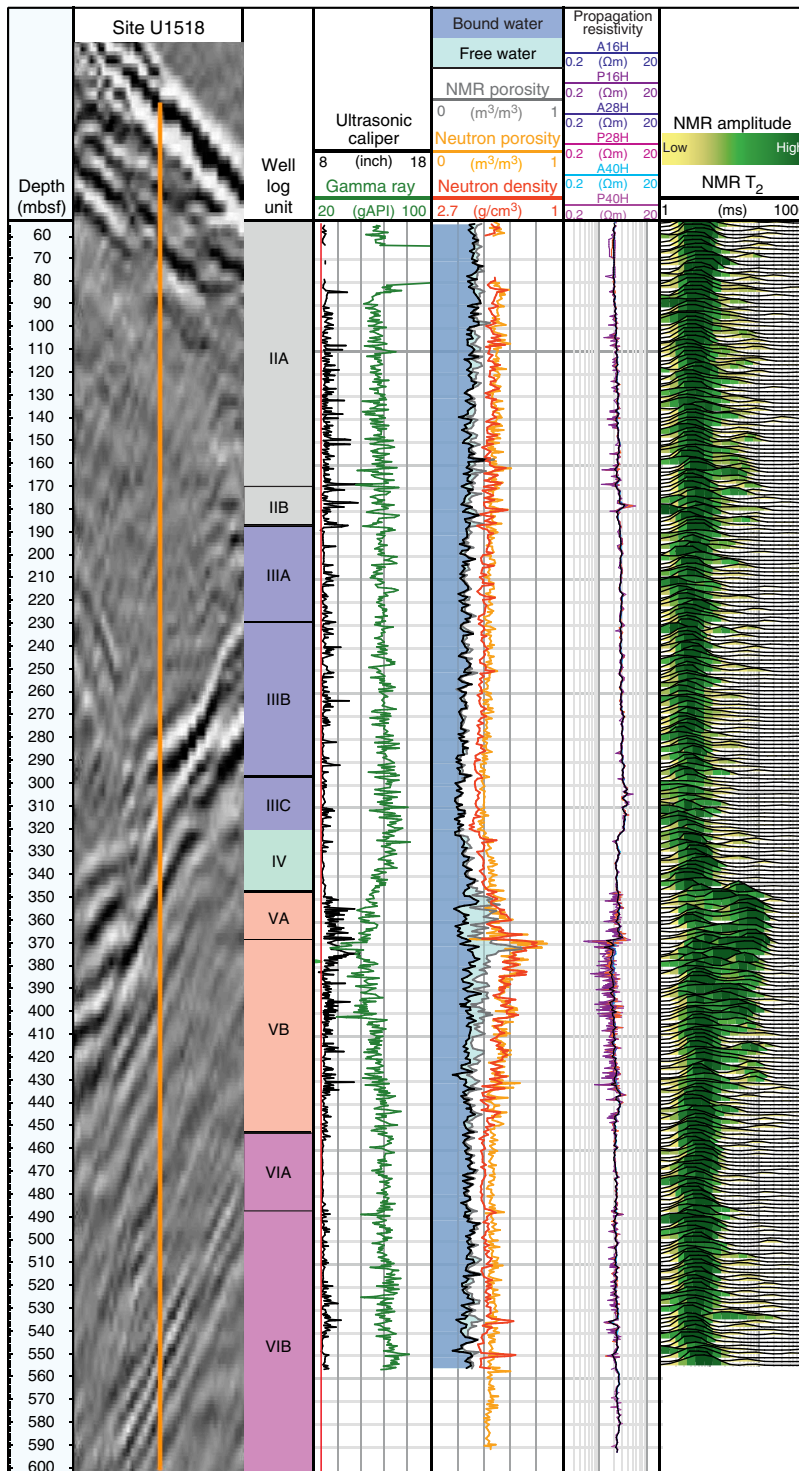




Figure F13. Composite plot of seismic image (05CM-04) and selected measurements from LWD, Site U1519. PSDM seismic section was provided by GNS Science, New Zealand.

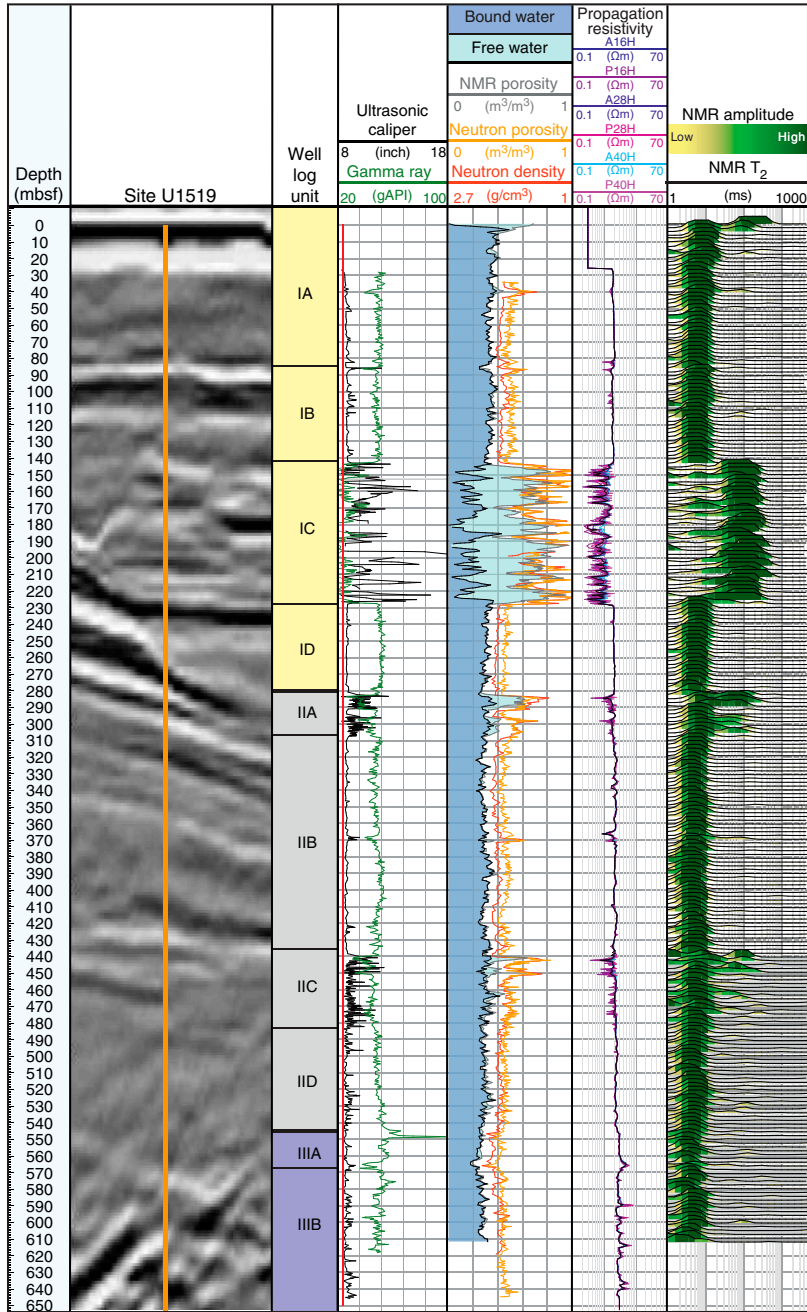


Figure F14. Composite plot of seismic image (05CM-04) and selected measurements from LWD, Site U1520. PSDM seismic section was provided by GNS Science, New Zealand.

